Hindawi
Advances in Astronomy
Volume 2021, Article ID 6698208, 25 pages
https://doi.org/10.1155/2021/6698208

*Research Article*

# Model of Charged Anisotropic Strange Stars in Minimally Coupled $f(R)$ Gravity

**H. Nazar and G. Abbas**

*Department of Mathematics, The Islamia University of Bahawalpur, Bahawalpur, Pakistan*

Correspondence should be addressed to G. Abbas; ghulamabbas@iub.edu.pk

Received 26 October 2020; Accepted 10 December 2020; Published 4 January 2021

Academic Editor: Kwing Lam Chan



In the present article, we have investigated a new family of nonsingular solutions of static relativistic compact sphere which incorporates the characteristics of anisotropic fluid and electromagnetic field in the context of minimally coupled $f(R)$ theory of gravity. The strange matter MIT bag model equation of state (EoS) has been considered along with the usual forms of the Karori–Barua (KB) metric potentials. For this purpose, we derived the Einstein–Maxwell field equations in the assistance of strange matter EoS and KB type ansatz by employing the two viable and cosmologically well-consistent models of $f(R) = R + \gamma R^2$ and $f(R) = R + \gamma R(R + \alpha R^2)$. Thereafter, we have checked the physical acceptability of the proposed results such as pressure, energy density, energy conditions, TOV equation, stability conditions, mass function, compactness, and surface redshift by using graphical representation. Moreover, we have investigated that the energy density and radial pressure are nonsingular at the core or free from central singularity and always regular at every interior point of the compact sphere. The numerical values of such parameters along with the surface density, charge to radius ratio, and bag constant are computed for three well-known compact stars such as (CS1)SAXJ1808.4 − 3658 ($\bar{x} = 7.07$ km), (CS2)VelaX − 1 ($\bar{x} = 9.56$ km), and (CS3)4U1820 − 30 ($\bar{x} = 10$ km) and are presented in Tables 1–6. Conclusively, we have noticed that our presented charged compact stellar object in the background of two well-known $f(R)$ models obeys all the necessary conditions for the stable equilibrium position and which is also perfectly fit to compose the strange quark star object.

## 1. Introduction

Several few decades ago, an intellectual thinking came in mind of research collaborators why our Universe is much rapidly growing towards large expansion. They tried to find out reasons behind this accelerating growth of Universe. Then, in 1990s, it was found that our Universe is expanding due to two hidden key factors of the nature, in which one of them is the theorized form of the matter known as dark matter and the other is unknown dark energy. Later on, the right picture of these factors was revealed by the international research collaboration team in 1998 by observing supernovae type-Ia [1–9], which was later proved by surveying of the cosmic microwave background (CMB) radiation [10, 11], huge scale structure [12–17], and Wilkinson Microwave Anisotropy Probe (WMAP) [18]. The above phenomenological factors of accelerating cosmic Universe can be well interpreted in higher order modified gravity theories rather than the concept of general relativity (GR) theory because these gravity theories could easily identify the right cosmological scenario of this mysterious Universe at the higher order curvature scale. For their assessment, several theoretical researchers and astrophysicists have contributed a quite exceptional work in different mathematical advances. To obtain these required mathematical setups, we can simply modify the Einstein–Hilbert action of GR corresponding to alternative theories of gravity such as $f(R)$ [19–22], $f(R,T)$ [23], $f(R,\mathcal{T},R_{\mu\nu}\mathcal{T}^{\mu\nu})$ [24–26], and $f(G)$ [27] gravity theories.

Exploring the physical stable configuration of relativistic stellar bodies, e.g., black hole, strange quark stars, pulsars, neutron stars, and white dwarfs in modified gravity theories,

would be a good task to grasp this issue at the theoretical and the astrophysical gauge for the researchers. In the massive stellar bodies, the analysis of huge gravitational attraction clearly defines the basic differences between GR and its alterations. The formation of huge dense star in an alternative $f(R)$ theory of gravity has included several fruitful characteristics to star models [28–36]. Psaltis [37] investigated that the huge gravitational field can be reviewed as modified theories of gravity. Briscese et al. [38] have proposed the stable position of objects in $f(R)$ gravity as a test of the theory's consistency. They reported that some paradigms of $f(R)$ gravity cannot maintain the stable position of star and are treated unreliable. From the analysis of Tsujikawa et al. [39], the unreliability regarding the stable position of these stellar bodies can be eluded due to scalar tensor theory. Despite of these outcomes, various concrete solutions have been made in the modeling of neutron stars by employing the $f(R)$ theory of gravity [40–48].

In the current investigation, we tried to find out new verity of nonsingular solutions of charged anisotropic relativistic compact stellar models in minimally coupled $f(R)$ gravity that were priory propounded by Alcock et al. [49] and Haensel et al. [50]. In regard to the existence of these objects, many attempts have been performed with different mechanisms during the last decade. Very recently, Shamir and Fayyaz [51] studied different properties of anisotropic compact celestial objects for Tolman–Kuchowicz spacetime by considering two viable classes of $f(R)$ models. The same author and his collaborators [52] determined the physical aspects of compact stellar bodies for KB line-element in modified $f(R,\phi)$ context. Yousaf et al. [53] investigated the impacts of different viable $f(R)$ paradigms on the existence of anisotropic stellar compact objects and found that these paradigms are well behaved at the astrophysical and the theoretical scales. The physical features of anisotropic spherically symmetric strange stars with quintessence field were discussed by Abbas et al. [54] for the specific pattern of the $f(R) = R + \lambda R^2$ model. Zubair and Abbas [55] found various realistic solutions of anisotropic interior compact celestial systems in the framework of $f(R)$ gravity. Sussman and Jaime [56] explored the viable characteristics of the $f(R) \propto \sqrt{R}$ model for nonstatic LTB spacetime in the presence of traceless anisotropic pressure tensor. Shabani and Ziaie [57] revealed the influence of the particular $f(R,T)$ model on the stability of an emerging Einstein Universe by employing the dynamical and numerical approaches. Garattini and Mandanici [58] proposed some equilibrium stable formations of different compact stellar systems and analyzed that additional higher order curvature terms emerging from rainbows gravity are likely to support different models of stellar systems. Several results of the anisotropic cosmic evolution in the background of different particular choices of $f(R,T)$ models were suggested by Sahoo et al. [59, 60]. From the literature survey, several phenomenal findings regarding these compact objects have been investigated in different alternative gravity theories with distinct approaches [61–69].

In spite of these consequences, several realistic features of anisotropic compact stellar systems have been examined in GR during the couple of few decades. Some notable exact solutions for the Einstein field equations with anisotropic source distributions in different backgrounds have been determined by Bayin [70], Cosenza et al. [71], and Harko and Mak [72, 73]. Mak and Harko [74] found a class of exact solutions of gravitational field equations for the physical existence of a compact object made of a strange quark matter. Kalam et al. [75, 76] proposed different analytical solutions of anisotropic compact stellar objects with KB spacetime. Hossein et al. [77] analyzed the physical aspects of the anisotropic celestial system in the presence of a cosmological constant. The analytical results of Einstein field equations describing the static anisotropic matter distributions of compact objects were examined by Bhar et al. [78, 79]. Very recently, the new family of exact solutions of the embedding class 1 method for relativistic anisotropic stellar bodies was explored by Singh et al. [80]. The same author and his collaborators [81] established new exact solutions of Tolman VII for anisotropic spherically symmetric compact star candidates in the presence of exotic matter nonlinear EoS. Various physical aspects of relativistic anisotropic compact celestial objects with the dark matter density profile were evaluated by Sarkar et al. [82]. Moreover, the physical realistic solutions of the DE profile for anisotropic relativistic compact stellar bodies were determined by Errehymy and Daoud [83].

The motivation for introducing an electromagnetic source in a matter distribution can be well justified in light of some theoretical manifests based on new techniques allowing for the appearance of a greater charge in relativistic compact celestial bodies. Particularly, there is a chance of an immense electromagnetic field in compact stellar bodies with a strange quark matter. A concerning problem emerges from the fact that, if star can hold a nonzero amount of charge, the contraction of such star can lead to a Reissner–Nordström black hole. A quite novel study presented by Rosseland [84] affirmed that the independent electrons of the extremely ionized gas that creates the star can be expelled due to its immense thermal velocities. In fact, a stellar body can hold a large value of electric charge maintaining stability [85, 86]. Rahaman et al. [87] studied several realistic properties of charged anisotropic compact objects with strange matter EoS. The embedding class 1 solutions of spherically symmetric compact stellar objects with charge distribution were investigated by Maurya et al. [88]. Thirukkanesh and Maharaj [89] concluded that the stability of a relativistic stellar object boost up with the infusion of an electric charge. Esculpi and Aloma [90] reported that the charge and anisotropy increases the stability of the object under certain bounds. Eiroa and Simeone [91] found that the electromagnetic field enhances the region of consistency for both shells and bubbles around a black hole.

The strange matter EoS based on the MIT bag model has a crucial role in the modeling of very massive dense strange quark stars. It has been foreseen that a neutron star is an end state of the gravitationally collapsed object which after consuming all its thermonuclear fuel comes into stabilized position by degenerating pressure. After a short period of the detection of the particle "neutron" by Chadwick, the

occurrence of neutron stars was forecasted. Subsequently, the notion got observational assistance with the detection of pulsars [92]. With the progress in our thinking of particle interaction at greater energy, theoretical composition of neutron stars has quite enhanced during the last few decades [93]. The speculation that the quark matter can be the most probable state of hadrons [94, 95] has focused to the debates of a complete new class of celestial objects composed of deconfined $u$, $d$, and $s$ quarks, generally says that strange quark stars.

According to above certain particulars, we have attempted to discuss the interior charged sphere distribution in the assistance of strange matter EoS within the $f(R)$ context. The realistic features of the physical parameters for the obtained solutions have been comprehensively studied, and its numerical estimation is also obtained. The arrangement of this manuscript as follows: in Section 2, the Einstein–Maxwell field equations for static anisotropic charged sphere case are formulated, and its corresponding solutions with central and surface values are also obtained. Section 3 deals with the unknown arbitrary constants that have been derived from the smooth matching conditions of the interior metric and exterior Reissner–Nordström solution. The estimated values of the physical parameters for our strange star candidates and their physical significance including energy conditions, TOV equation, anisotropy, and stability conditions are thoroughly discussed in Sections 4 and 5, respectively. In subsequent section, we have examined various physical profiles such as effective gravitational mass, compactification factor, and surface redshift for our presented star candidate. Finally, Section 7 comprises the final remarks for our present strange star candidate.

## 2. Charged Interior Anisotropic Matter Configuration

We considered the static spherically symmetric strange star configuration which is bounded by interiorly charged anisotropic source distribution within the framework of so-called $f(R)$ gravity theory. The general formulation of Einstein–Hilbert (EH) action in GR is expressed by

$$S_{\mathrm{EH}} = \frac{1}{2\kappa}\int d^4x\sqrt{-g}R. \tag{1}$$

The above action in metric $f(R)$ formalism with minimally coupled Maxwell source has the following form:

$$S_{\mathrm{mod}+M} = \frac{1}{2}\int d^4x\sqrt{-g}\left(\frac{f}{\kappa} - \frac{\mathrm{F}}{2\pi}\right), \tag{2}$$

where $\mathscr{F} = (1/4)F_{\tau\nu}F^{\tau\nu}$ determines the role of Maxwell invariant, $f = f(R)$ corresponds to the generic function of Ricci scalar $R$, and $\kappa$ represents the coupling constant. Therefore, the set of $f(R)$ field equations can be acquired by the variation of equation (2) w.r.t metric tensor:

$$\left(g_{\chi\psi}\Box - \nabla_\chi\nabla_\psi + R_{\chi\psi}\right)F(R) - \frac{1}{2}f(R)g_{\chi\psi} = \kappa\left(T_{\chi\psi} + \mathrm{E}_{\chi\psi}\right). \tag{3}$$

Here, $\mathbb{E}_{\chi\psi}$ is an electromagnetic tensor, $T_{\chi\psi}$ indicates an energy-momentum tensor, $F(R) = (\mathrm{d}f/\mathrm{d}R)$ is the derivative function of Ricci scalar $R$, $\Box$ corresponds to the D'Alembert operator, and $\nabla_\chi$ stands for the covariant derivative. The above equation can be rearranged in the form of Einstein tensor which yield as

$$G_{\chi\psi} = \frac{1}{F}\left(\kappa\mathrm{H}_{\chi\psi}\right), \tag{4}$$

where $\mathbb{H}_{\chi\psi} = \mathbb{E}_{\chi\psi} + T_{\chi\psi} + T^D_{\chi\psi}$ with

$$T^D_{\chi\psi} = \frac{1}{\kappa}\left[\left(\nabla_\chi\nabla_\psi - g_{\chi\psi}\Box\right)F(R) + \frac{g_{\chi\psi}}{2}\left(f - RF(R)\right)\right]. \tag{5}$$

The role of $T^D_{\chi\psi}$ as an effective energy-momentum tensor arrives from the theory parameter, which literally describes that the nature of dark energy correlates with early and late time accelerating expansions of the cosmic Universe in the gravitational system. In other words, this $T^D_{\chi\psi}$ factor expresses the fourth order differential geometry to identify the huge curvature at the astrophysical and cosmological backgrounds. Now, we presume the interior static strange star distribution defined by the KB [96] line-element and is given by

$$\mathrm{d}s^2 = -e^{\zeta}\mathrm{d}t^2 + e^{\xi}\mathrm{d}r^2 + r^2\left(\mathrm{d}\theta^2 + \sin^2\theta\mathrm{d}\phi^2\right), \tag{6}$$

where $\zeta = \zeta(r)$ and $\xi = \xi(r)$ are the two metric variables that depend on $r$ function and positively assumed. It is equivalent to the KB type solutions where $\zeta = \tilde{Y}r^2 + \tilde{Z}$ and $\xi = \tilde{X}r^2$. Thus, $\tilde{X}$, $\tilde{Y}$, and $\tilde{Z}$ are the arbitrary constants and would be investigated later through matching conditions. The Einstein–Maxwell field equations can be arranged with the help of equations (3) and (6) by employing $c = G = 1$ and read by

$$\left(\frac{\xi'}{r} - \frac{1}{r^2}\right)e^{-\xi} + \frac{1}{r^2} = \left(\mu + \frac{\mathbb{E}^2}{8\pi}\right)\frac{8\pi}{F} + \frac{1}{F}\left[\frac{f - RF}{2} + e^{-\xi}\left(\left(\frac{2}{r} - \frac{\xi'}{2}\right)F' + F''\right)\right], \tag{7}$$

$$\left(\frac{\zeta'}{r} + \frac{1}{r^2}\right)e^{-\xi} - \frac{1}{r^2} = \left(P_r - \frac{\mathbb{E}^2}{8\pi}\right)\frac{8\pi}{F} - \frac{1}{F}\left[\frac{f - RF}{2} + F'e^{-\xi}\left(\frac{\zeta'}{2} + \frac{2}{r}\right)\right], \tag{8}$$

$$\frac{1}{4}\left[2\frac{\zeta'-\xi'}{r}-\xi'\zeta'+\zeta'^2+2\zeta''\right]e^{-\xi} =\left(P_t+\frac{\mathbb{E}^2}{8\pi}\right)\frac{8\pi}{F}-\frac{1}{F}\left[\frac{f-RF}{2}+e^{-\xi}\left(\left(\frac{1}{r}+\frac{\zeta'}{2}-\frac{\xi'}{2}\right)F'+F''\right)\right], \tag{9}$$

$$\mathbb{E}(r)=\frac{q(r)}{r^2}, \tag{10}$$

where $q(r)=4\pi\int_0^r \rho r^2 e^{(\xi/2)}\mathrm{d}r$ signifies the total charge inside the matter spheroid of radius $r$. The following specific MIT bag model EoS [49, 94, 95, 97, 98] determines the strange matter distribution in the interior celestial object and is read as

$$P_r=\frac{1}{3}\left(\mu-4B_g\right). \tag{11}$$

Here, $B_g$ is defined as the bag constant. The difference between the bag constant and mass density of the perturbed and nonperturbed QCD vacuum was investigated by Mak and Harko [74], and the units of bag constant Mevfm$^{-3}$ is derived by Chodos et al. [98].

*2.1. Solution of Modified Field Equations.* There are five independent equations together with above EoS given in five unknowns, namely, energy density $\mu(r)$, pressures ($P_r$ and $P_t$), electric field $\mathbb{E}(r)$, and proper charge density $\rho(r)$. The solution sets of these unknown parameters are determined from equations (7)–(11); by implementing the KB type ansatz $\zeta=\widetilde{Y}r^2+\widetilde{Z}$ and $\xi=\widetilde{X}r^2$, it becomes

$$\begin{aligned}
\mu&=\frac{3e^{-\widetilde{X}r^2}}{16\pi}\left[F(\widetilde{X}+\widetilde{Y})+\frac{1}{2}\{(\widetilde{X}+\widetilde{Y})rF'-F''\}\right]+B_g,\\
P_r&=\frac{e^{-\widetilde{X}r^2}}{16\pi}\left[F(\widetilde{X}+\widetilde{Y})+\frac{1}{2}\{(\widetilde{X}+\widetilde{Y})rF'-F''\}\right]-B_g,\\
P_t&=\frac{1}{8\pi}\left[\left\{\left(\frac{7\widetilde{Y}}{2}-\frac{3\widetilde{X}}{2}-r^2\widetilde{X}\widetilde{Y}+r^2\widetilde{Y}^2+\frac{1}{r^2}\right)e^{-\widetilde{X}r^2}-\frac{1}{r^2}\right\}F+\left\{(f-RF)+e^{-\widetilde{X}r^2}\left(\left(\frac{7r\widetilde{Y}}{4}-\frac{5r\widetilde{X}}{4}+\frac{3}{r}\right)F'+\frac{5F''}{4}\right)\right\}\right]+B_g,\\
\mathbb{E}^2&=\left[\frac{1}{2}\left(\widetilde{X}-3\widetilde{Y}-\frac{2}{r^2}\right)e^{-\widetilde{X}r^2}+\frac{1}{r^2}\right]F+\frac{1}{2}\left[-(f-RF)+e^{-\widetilde{X}r^2}\left(\left(\frac{r\widetilde{X}}{2}-\frac{3r\widetilde{Y}}{2}-\frac{4}{r}\right)F'-\frac{F''}{2}\right)\right]-8\pi B_g,
\end{aligned} \tag{12}$$

while the charge density is evaluated as

$$\begin{aligned}
\rho=\frac{e^{-\left(3\widetilde{X}r^2/2\right)}}{16\pi r^3\sqrt{\varphi}}\Big[&4F\left\{-2+2e^{\widetilde{X}r^2}+2r^2(2\widetilde{X}-3\widetilde{Y})-r^4\widetilde{X}(\widetilde{X}-3\widetilde{Y})\right\}-2re^{\widetilde{X}r^2}\Big\{-2F'\\
&+r\left(4(f-RF)+64\pi B_g+r(f-RF)'\right)\Big\}-r\Big\{\Big(28+r^2(-23\widetilde{X}+21\widetilde{Y})+2r^4\widetilde{X}(\widetilde{X}-3\\
&\times\widetilde{Y})\Big)F'+r\left(3\left(4+r^2(\widetilde{Y}-\widetilde{X})\right)F''+rF'''\right)\Big\}\Big],
\end{aligned} \tag{13}$$

where

$$\varphi = \frac{e^{-\widetilde{X}r^2}}{r^2}\left[2F\left\{-2+2e^{\widetilde{X}r^2}+r^2\left(\widetilde{X}-3\widetilde{Y}\right)\right\}+r\left\{-8F'+r\left(-2e^{\widetilde{X}r^2}\left((f-RF)+16\pi B_g\right)\right.\right.\right.$$
$$\left.\left.\left.+rF'\left(\widetilde{X}-3\widetilde{Y}\right)-F''\right)\right\}\right]. \tag{14}$$

The total charge within a compact sphere of radius $r$ becomes

$$q = r^2\sqrt{\frac{Fe^{-\widetilde{X}r^2}}{2}\left(\widetilde{X}-3\widetilde{Y}-\frac{2}{r^2}\right)+\frac{F}{r^2}-\frac{1}{2}\left[(f-RF)-e^{-\widetilde{X}r^2}\left(\left(\frac{r\widetilde{X}}{2}-\frac{3r\widetilde{Y}}{2}-\frac{4}{r}\right)F'-\frac{F''}{2}\right)\right]-8\pi B_g}. \tag{15}$$

*2.2. Constraints on Physical Parameters.* To examine the regular value (from central singularity free) at the core of the strange stars models for the physical acceptability of energy density $(\mu)$ and pressure $(P_r)$. These physical parameters are analyzed in the form of analytical expressions and are given by

$$\mu(0) = \frac{3}{16\pi}\left[\left(\widetilde{X}+\widetilde{Y}\right)F-\frac{F''}{2}\right]+B_g, \tag{16}$$

$$P_r(0) = \frac{1}{16\pi}\left[\left(\widetilde{X}+\widetilde{Y}\right)F-\frac{F''}{2}\right]-B_g. \tag{17}$$

The above solutions ($\mu(0)$ and $P_r(0)$) are free of central singularity and finite (regular) at the core of the different strange star candidates. There is also nonnegative behavior and maximum position at the center of the compact sphere. The numerical values of the said parameters are provided in Tables 1–6 for three different strange stars ((CS1) SAXJ1808.4 − 3658 ($\widetilde{x} = 7.07$ km), (CS2) Vela$X-1$ ($\widetilde{x} = 9.56$ km), and (CS3) $4U1820-30$ ($\widetilde{x} = 10$ km)) with two cosmologically prominent viable $f(R)$ models. Moreover, at the core of compact sphere, the electric field $(\mathbb{E})$ must disappear for the requirement of regularity condition. The regularity of the electric field turned out to be

$$0 = \mathbb{E}^2(0) = \frac{3F}{2}\left(\widetilde{X}-\widetilde{Y}\right)-\frac{1}{2}\left((f-RF)+\frac{9F''}{2}\right)-8\pi B_g. \tag{18}$$

From the above result, we obtain the value of the bag constant $B_g$.

$$B_g = \frac{3F}{16\pi}\left(\widetilde{X}-\widetilde{Y}\right)-\frac{1}{16\pi}\left((f-RF)+\frac{9F''}{2}\right). \tag{19}$$

We used the value of the bag constant $(B_g)$ in equation (16) and then obtained the parameter $\widetilde{X}$ in terms of the central density and modified $f(R)$ terms which is expressed by

$$\widetilde{X} = \frac{1}{F}\left[\frac{8\pi\mu(0)}{3}+\frac{(f-RF)}{6}+F''\right]. \tag{20}$$

The numerical values of $B_g$ are provided in Tables 1–6 for three distinct strange star candidates through two different viable $f(R)$ models for the values of free parameter $\gamma$.

## 3. Matching Conditions

We explore the three unknown arbitrary constants in terms of $M$, $R$, and $Q$ by imposing the smooth matching conditions between the interior spacetime and exterior Reissner–Nordström solution at the bounding three-surface $r = \widetilde{x}$ (where $\widetilde{x} > 2M$) of the fluid sphere. Both interior and exterior metrics at the bounding hypersurface must be continuous. Hence, the exterior line-element of the spherical star was well depicted by the Reissner–Nordström solution [99, 100] and is expressed by

$$ds^2 = -\left(1-\frac{2M}{r}+\frac{Q^2}{r^2}\right)dt^2+\left(1-\frac{2M}{r}+\frac{Q^2}{r^2}\right)^{-1}dr^2$$
$$+r^2\left(d\theta^2+\sin^2\theta d\phi^2\right), \tag{21}$$

where $Q$, $M$, and $r = \widetilde{x}$ are the total charge surrounded within a bounding three-surface, the total mass of the gravitational system, and the radius at the bounding hypersurface (i.e., where exterior and interior spacetimes are smoothly matched). The continuity of the gravitational potentials $g_{rr}$, $g_{tt}$, and $(\partial g_{tt}/\partial r)$ across the junction interface $r = \widetilde{x}$ between the exterior and interior geometries of the sphere provides the following expressions:

$$\left(1-\frac{2M}{\widetilde{x}}+\frac{Q^2}{\widetilde{x}^2}\right) = e^{\widetilde{Y}\widetilde{x}^2+\widetilde{Z}}, \tag{22}$$

$$\left(1-\frac{2M}{\widetilde{x}}+\frac{Q^2}{\widetilde{x}^2}\right)^{-1} = e^{\widetilde{X}\widetilde{x}^2}, \tag{23}$$

$$\left(\frac{M}{\widetilde{x}^2}-\frac{Q^2}{\widetilde{x}^3}\right) = \widetilde{Y}\widetilde{x}e^{\widetilde{Y}\widetilde{x}^2+\widetilde{Z}}. \tag{24}$$

The resulting expressions (22)–(24) yield the following outcomes for the arbitrary unknown constant parameters:

Table 1: Computed values of the physical parameters, namely, matter density, radial pressure, total charge, bag constant, and their unknown arbitrary constants ($\tilde{X}$, $\tilde{Y}$, and $\tilde{Z}$) for the CS1 candidate with the viable model $f(R) = R + \gamma R^2$, in which we assume $\gamma$ is the free constant parameter of the proposed model.

| $\gamma$ | $\tilde{X}(\mathrm{km}^{-2})$ | $\tilde{Y}(\mathrm{km}^{-2})$ | $\tilde{Z}(\mathrm{km}^{-2})$ | $(Q^2/\tilde{x}^2)$ | $B_g(\mathrm{km}^{-2})$ | $\mu(0)(10^{15})(\mathrm{gm/cm}^3)$ | $\mu(\tilde{x})(10^{15})(\mathrm{gm/cm}^3)$ | $P_r(0)(10^{35})(\mathrm{dyne/cm}^2)$ |
|---|---|---|---|---|---|---|---|---|
| 0.1 | 0.01702 | 0.01282 | −1.4915 | 0.0258 | 0.0002543 | 2.7414811 | 1.3671234 | 4.1084432 |
| 0.2 | 0.01708 | 0.01291 | −1.4989 | 0.0246 | 0.0002559 | 2.7556953 | 1.3713454 | 4.1252010 |
| 0.3 | 0.01714 | 0.01300 | −1.5064 | 0.0234 | 0.0002571 | 2.7693707 | 1.3750069 | 4.1443929 |

Table 2: Values of the unknown constant parameters, bag constant, and physical parameters are calculated for the CS1 object by using the well-known model $f(R) = R + \gamma R(R + \alpha R^2)$, in which $\alpha$ is the fixed constant number and $\gamma$ is the free parameter of the suggested model (where $\alpha = 0.5$).

| $\gamma$ | $\tilde{X}$ $(\mathrm{km}^{-2})$ | $\tilde{Y}$ $(\mathrm{km}^{-2})$ | $\tilde{Z}$ $(\mathrm{km}^{-2})$ | $(Q^2/\tilde{x}^2)$ | $B_g$ $(\mathrm{km}^{-2})$ | $\mu(0)(10^{15})$ $(\mathrm{gm/cm}^3)$ | $\mu(\tilde{x})(10^{15})$ $(\mathrm{gm/cm}^3)$ | $P_r(0)(10^{35})$ $(\mathrm{dyne/cm}^2)$ |
|---|---|---|---|---|---|---|---|---|
| 0.1 | 0.017027 | 0.012824 | −1.49211 | 0.0257 | 0.0002546 | 2.7427695 | 1.3675466 | 4.1074605 |
| 0.2 | 0.017083 | 0.012916 | −1.49955 | 0.0245 | 0.0002558 | 2.7562841 | 1.3713648 | 4.1285794 |
| 0.3 | 0.017139 | 0.013009 | −1.50702 | 0.0233 | 0.0002566 | 2.7693403 | 1.3746579 | 4.1547818 |

Table 3: Estimated values of the bag constant, physical parameters, and their unknown constants for the (CS2) candidate through the proposed model $f(R) = R + \gamma R^2$.

| $\gamma$ | $\tilde{X}$ $(\mathrm{km}^{-2})$ | $\tilde{Y}$ $(\mathrm{km}^{-2})$ | $\tilde{Z}$ $(\mathrm{km}^{-2})$ | $(Q^2/\tilde{x}^2)$ | $B_g$ $(\mathrm{km}^{-2})$ | $\mu(0)(10^{15})$ $(\mathrm{gm/cm}^3)$ | $\mu(\tilde{x})(10^{14})$ $(\mathrm{gm/cm}^3)$ | $P_r(0)(10^{35})$ $(\mathrm{dyne/cm}^2)$ |
|---|---|---|---|---|---|---|---|---|
| 0.1 | 0.00834 | 0.00610 | −1.3201 | 0.0128 | 0.0001350 | 1.3427257 | 7.2354488 | 1.8435704 |
| 0.2 | 0.00835 | 0.00612 | −1.3228 | 0.0123 | 0.0001356 | 1.3459457 | 7.2498261 | 1.8435321 |
| 0.3 | 0.00837 | 0.00614 | −1.3261 | 0.0117 | 0.0001368 | 1.3507778 | 7.2710506 | 1.8386382 |

Table 4: Numerical values of the physical parameters, bag constant, and unknown arbitrary constants calculated from the CS2 candidate by implementing a viable model $f(R) = R + \gamma R(R + \alpha R^2)$ for different values of free parameter $\gamma$ and $\alpha = 0.5$.

| $\gamma$ | $\tilde{X}$ $(\mathrm{km}^{-2})$ | $\tilde{Y}$ $(\mathrm{km}^{-2})$ | $\tilde{Z}$ $(\mathrm{km}^{-2})$ | $(Q^2/\tilde{x}^2)$ | $B_g$ $(\mathrm{km}^{-2})$ | $\mu(0)(10^{15})$ $(\mathrm{gm/cm}^3)$ | $\mu(\tilde{x})(10^{14})$ $(\mathrm{gm/cm}^3)$ | $P_r(0)(10^{35})$ $(\mathrm{dyne/cm}^2)$ |
|---|---|---|---|---|---|---|---|---|
| 0.1 | 0.008339 | 0.006102 | −1.31995 | 0.01283 | 0.0001347 | 1.3424020 | 7.2322780 | 1.8474434 |
| 0.2 | 0.008353 | 0.006123 | −1.32297 | 0.01228 | 0.0001356 | 1.3464280 | 7.2505875 | 1.8449772 |
| 0.3 | 0.008365 | 0.006143 | −1.32594 | 0.01174 | 0.0001363 | 1.3499435 | 7.2660481 | 1.8442099 |

Table 5: Values of the unknown constants, bag constant, and physical parameters computed from the (CS3) object by using the well-known model $f(R) = R + \gamma R^2$ for different choices of free parameter $\gamma$.

| $\gamma$ | $\tilde{X}$ $(\mathrm{km}^{-2})$ | $\tilde{Y}$ $(\mathrm{km}^{-2})$ | $\tilde{Z}$ $(\mathrm{km}^{-2})$ | $(Q^2/\tilde{x}^2)$ | $B_g$ $(\mathrm{km}^{-2})$ | $\mu(0)(10^{15})$ $(\mathrm{gm/cm}^3)$ | $\mu(\tilde{x})(10^{14})$ $(\mathrm{gm/cm}^3)$ | $P_r(0)(10^{35})$ $(\mathrm{dyne/cm}^2)$ |
|---|---|---|---|---|---|---|---|---|
| 0.1 | 0.00958 | 0.00742 | −1.7017 | 0.0471 | 0.00012959 | 1.5412454 | 6.9890067 | 2.5256667 |
| 0.2 | 0.00960 | 0.00745 | −1.7060 | 0.0465 | 0.00012961 | 1.5452920 | 6.9941908 | 2.5374675 |
| 0.3 | 0.00962 | 0.00748 | −1.7103 | 0.0459 | 0.00012958 | 1.5492713 | 6.9986608 | 2.5498737 |

Table 6: Values of the bag constant, unknown arbitrary constants, and physical parameters are computed from the CS3 candidate through the proposed viable model $f(R) = R + \gamma R(R + \alpha R^2)$.

| $\gamma$ | $\tilde{X}$ $(\mathrm{km}^{-2})$ | $\tilde{Y}$ $(\mathrm{km}^{-2})$ | $\tilde{Z}$ $(\mathrm{km}^{-2})$ | $(Q^2/\tilde{x}^2)$ | $B_g$ $(\mathrm{km}^{-2})$ | $\mu(0)(10^{15})$ $(\mathrm{gm/cm}^3)$ | $\mu(\tilde{x})(10^{14})$ $(\mathrm{gm/cm}^3)$ | $P_r(0)(10^{35})$ $(\mathrm{dyne/cm}^2)$ |
|---|---|---|---|---|---|---|---|---|
| 0.1 | 0.009587 | 0.007427 | −1.70143 | 0.04714 | 0.0001296 | 1.5423844 | 6.9897874 | 2.5289177 |
| 0.2 | 0.009604 | 0.007456 | −1.70595 | 0.04651 | 0.0001295 | 1.5459478 | 6.9936871 | 2.5412079 |
| 0.3 | 0.009621 | 0.007486 | −1.71069 | 0.04585 | 0.0001293 | 1.5494569 | 6.9965141 | 2.5549496 |

$$\widetilde{X} = \frac{-1}{\widetilde{x}^2}\ln\left(1 - \frac{2M}{\widetilde{x}} + \frac{Q^2}{\widetilde{x}^2}\right),$$

$$\widetilde{Y} = \frac{1}{\widetilde{x}^2}\left(\frac{M}{\widetilde{x}} - \frac{Q^2}{\widetilde{x}^2}\right)\left(1 - \frac{2M}{\widetilde{x}} + \frac{Q^2}{\widetilde{x}^2}\right)^{-1},$$

$$\widetilde{Z} = \ln\left(1 - \frac{2M}{\widetilde{x}} + \frac{Q^2}{\widetilde{x}^2}\right) - \left(\frac{M}{\widetilde{x}} - \frac{Q^2}{\widetilde{x}^2}\right)\left(1 - \frac{2M}{\widetilde{x}} + \frac{Q^2}{\widetilde{x}^2}\right)^{-1}. \tag{25}$$

Consequently, we found the solutions of these unknown parameters $\widetilde{X}$, $\widetilde{Y}$, and $\widetilde{Z}$ in the form of total charge $Q$, mass $M$, and radius $\widetilde{x}$ for our proposed different strange stars which are quite suitable to describe the graphical evolution. The approximated numerical values of these unknown parameters for three different strange star candidates (CS1)SAXJ1808.4 − 3658 ($\widetilde{x} = 7.07$ km), (CS2)Vela$X-1$ ($\widetilde{x} = 9.56$ km), and (CS3)$4U1820-30$ ($\widetilde{x} = 10$ km) with two distinct viable $f(R)$ models are given in Tables 1–6. Here, it would be very necessary to examine the analytical expression of the charge $Q$ of the strange star. So, we employed the above equations on the system constraint and is given by

$$\begin{aligned}
&\frac{1}{\widetilde{x}^2\left(\widetilde{x}^2 - 2M\widetilde{x} + Q^2\right)}\Big[\left(-4 + 2F - \widetilde{x}\left(5F' + \widetilde{x}F''\right)\right)Q^4 + \widetilde{x}Q^2\Big\{\Big(8 - 2F + 23\widetilde{x}F' + 4\widetilde{x}^2F''\Big)M \\
&+ \widetilde{x}\Big(-4 - 4F - 13\widetilde{x}F' + 7\widetilde{x}^2F''\Big)\Big\} + \widetilde{x}^2\{-4(M - 2\widetilde{x})MF - \widetilde{x}(2M - \widetilde{x})\left((13M - 8\widetilde{x})F'\right. \\
&\left.+ 2\widetilde{x}F''(M + 4\widetilde{x})\right)\} - \Big(\widetilde{x}^2 - 2M\widetilde{x} + Q^2\Big)\Big(\Big(\widetilde{x}^2 - 2M\widetilde{x} + Q^2\Big)\widetilde{x}F' + 2F\Big(-2\widetilde{x}^2 - 2M\widetilde{x} + Q^2\Big)\Big) \\
&\times\ln\left[\frac{\left(\widetilde{x}^2 - 2M\widetilde{x} + Q^2\right)}{\widetilde{x}^2}\right]\Big] = 0.
\end{aligned} \tag{26}$$

Alternatively, we obtained the numerically solved estimated value of the above result to the ratio of charge and radius ($Q/\widetilde{x}$) for the given compactness ($M/\widetilde{x}$) of star. In spite of this condition, there is another estimation that should be validated between the charge radius ratio and the compactness as $((Q^2/\widetilde{x}^2) < (2M/\widetilde{x}))$. The maximum allowable limit of the charge to radius ratio ($Q^2/\widetilde{x}^2$) is given in Tables 1–6 for different celestial objects with two well-known $f(R)$ models for different choices of free parameter $\gamma$. These numerical estimated values signify that our presented celestial objects are very capable to be strange stars instead of neutron stars.

## 4. Analysis of Physically Estimated Values

Since we have examined the physical bounds of the compact stars along with their corresponding unknown parameters that are well-consistent to our standard observational data, we noticed from this investigation that the compactification of the star is greater than that of a neutron star. This analysis would be very fruitful to obtain an estimation of the physical reliable results, namely, matter density, pressure, charge to radius ratio, and the bag constant. We studied compact star candidates of distinct compactness and computed the relevant unknown constant parameters. The numerical values are given in Tables 1–7. For instance, we observed the estimated values of CS1 candidate of mass $1.435M_\odot$ and radius $\widetilde{x} = 7.07$ km in the background of the viable model $f(R) = R + \gamma R^2$ for the value of $\gamma = 0.1$, and the numerical values of the unknowns are gained as $\widetilde{X} = 0.01702$, $\widetilde{Y} = 0.01282$, and $B_g = 0.0002543$ in units of $(1/\text{km}^2)$ and $Q^2/R^2 = 0.0258$. Substituting the values of $c$ and $G$ into the corresponding expressions, afterwards, the values of the physical parameters and the bag constant are $\mu(0) = 2.7414811 \times 10^{15}\,(\text{g/cm}^3)$, $\mu(\widetilde{x}) = 1.3671234 \times 10^{15}\,(\text{g/cm}^3)$, $P_r(0) = 4.1084432\,(\text{dyne/cm}^2)$, and $B_g = 192.157\,(\text{MeV/fm}^3)$, respectively. Note that for the next increasing values of $\gamma$, the corresponding values of the unknowns, energy density, pressure, and bag constant increase, but the value of charge to radius ratio decreases (Table 1). At similar fashion, one can also check the values of these physical parameters against another well-known viable model $f(R) = R + \gamma R(R + \alpha R^2)$. From the constraint of equation (26), the minimum value of the charge to radius ratio is 0.0128 against the minimum compactness = 0.273 of the given star data. Hence, for the star of mass $1.77M_\odot$, the relevant maximal radius is $\widetilde{x} = 9.56$ km. For the feasible reliable investigation of the physical parameters at the interior of the celestial object, we have considered the CS1 object and drawn different evolutions of the matter density, pressures (radial and tangential), electric field, energy conditions, equilibrium equation, and stability parameters.

Moreover, in this scenario, the value of $B_g$ escalates with the increment of the compactness (i.e., $B_g$ is the density reliant). An ultradense object wants maximum $B_g$. The corresponding attentions were determined in [101], where a density-reliant $B_g$ has been considered to paradigm magnetized strange quark structures. To continue this description, the leading motivation of Farhi and Jaffe [95] presented that for the stable strange matter configuration and estimated that the $B_g$ must encompass nearly $60\,\text{MeV/fm}^{-3}$. In comparison of these results, our outcomes indicate that with

Table 7: The observational data of the radii, masses, and compactifications for the three well-known compact objects ((CS1) SAXJ1808.4 − 3658, (CS2) Vela$X$ − 1, and (CS3) 4$U$1820 − 30). We proposed our study with CS1 candidate to describe the physical importance as well as their graphical representation.

| Compact stars | $\tilde{x}$ (km) | $M(M_\odot)$ | Mass (km) | $(M/\tilde{x})$ | $(2M/\tilde{x})$ |
|---|---|---|---|---|---|
| SAXJ1808.4 − 3658 | 7.07 | 1.435 | 2.1166 | 0.299 | 0.598 $<(8/9)$ |
| Vela$X$ − 1 | 9.56 | 1.77 | 2.6108 | 0.273 | 0.546 $<(8/9)$ |
| 4$U$1820 − 30 | 10 | 2.25 | 3.3188 | 0.331 | 0.662 $<(8/9)$ |

the incorporation of electromagnetic charge and anisotropy, $B_g$ returns in a greater value. In regard of the study by Farhi and Jaffe [95], the investigation was identified for a $\beta$-stable strange quark matter fulfilling the baryon number conservation principle where the uncharged state was considered. The framework of stability was constituted by three factors such as $B_g$, the mass of the quark particles, and the QCD coupling constant. What comes off if the uncharge state is not implemented is not clear from the study. For a likely immense strange quark matter, there might be a gathering of an absolute positive charge in the interior of the object. Perhaps, in the inclusion of electric charge, to resist the directed outward force produced due to the electromagnetic field, the bag pressure escalates. The point, although, is a problem of more analysis. Thus, when one wants to employ a mathematical consistent and physically reliable exact result to paradigm strange objects, the $B_g$ does not carry a constant. Therefore, it becomes a free parameter that depends on the compactification of the object.

## 5. Physical Aspects of the CS1 Object

*5.1. Evolution of Matter Density, Pressure, and Electric Field.* In this conjecture, we described suitable aspects of the various physical parameters, namely, energy density, radial and transverse pressures, electric field, and derivative function of the energy density and radial pressure for the proposed CS1 candidate in the background of two popular and cosmologically viable classes of $f(R)$ models. These types of feasible models are $f(R) = R + \gamma R^2$ [102] and $f(R) = R + \gamma R(R + \alpha R^2)$ [42], in which one of them is recognized as quadratic curvature formulation of the generic function of Ricci scalar $R$ and the other is the modified form of the prior model in terms of cubic corrections. Several reasonable outcomes of these models have been devoted in the literature [53, 103–106] for the physical evaluation of the collapsing star and the stable equilibrium condition of the star at the theoretical as well as the astrophysical backgrounds.

It would be very necessary to discuss on the role of model parameters because they should be quite consistent and right for the stable formation of the interior celestial object. Besides other unknown parameters, these are considered as initial parameters and govern the physical aspects and their graphical evolution of the stable object. Hence, in our first suggested paradigm $f(R) = R + \gamma R^2$, the value of $\gamma$ is considered as 0.1–0.3 at equal intervals of units, and this similar approach was used for the model $f(R) = R + \gamma R$ $(R + \alpha R^2)$, in which $\alpha = 0.5$.

To obtain the stable configuration of the compact star, there are several feasible features available from which first we analyze matter density and radial and transverse pressures for their physical credibility and graphical evolution. These said parameters must be free of central singularity or regular at the core of the interior compact stellar object as well as nonnegative throughout the whole distribution. Also, the nature should be maximum around the center where $\tilde{x} = 0$ and minimum at the boundary surface of the sphere where $r = \tilde{x}$. The derivatives of the matter density and radial pressure are monotonically decreasing functions of $r$, i.e., their evolution satisfies the bound $0 < r < \tilde{x}$.

The evolution of the energy density with their respective $f(R)$ models for the interior compact object is studied and shown in Figure 1. It is seen from Figure 1 that each plot of the energy density shows nonnegative nature within the entire region of the star, and it suggests maximum behavior at the center and minimum towards the boundary surface of the sphere. Apart from this description, one important point to discuss is that the numerical value of the central density is up most in competition of the surface density of the compact star candidates (Tables 1–6), which is actually the property of massive strange quark stellar objects [107–110]. Figures 2 and 3 show the evolutionary nature of the radial and transverse pressures through graphical analysis by using two well-known $f(R)$ models. One can easily understand from Figures 2 and 3 that the radial and tangential pressures with their respective $f(R)$ models represent positive evolution in the entire distribution of the star and indicate the utmost regular behavior at the core of the star but low most at the boundary surface where $r = \tilde{x}$. In particular, we note that the radial pressure sharply dies out at the boundary sphere [111], but transverse pressure does not disappears promptly at the surface of the sphere which displays the spheroidal nature of the strange celestial star [112–114]. Figure 4 shows the distribution of the derivative function of energy density and radial pressure by employing the numerical values of different unknown parameters. It can be eminently seen from Figure 4 that both combined plots with their respective $f(R)$ models indicate monotonically decreasing nature within the entire region of the sphere, i.e., they possess negative behavior at the interior of the star. Moreover, we plot the evolution of the electric field for the proposed CS1 object with two viable $f(R)$ models (Figure 5). The evolutionary behavior of the electric field in each respective plot suggests positive nature and increases with the increase of $r$ of the celestial star.

*5.2. Equation of State.* We shed light over the results of EoS parameters for the presented interior CS1 candidate with two prominent and cosmologically viable $f(R)$ models. Various consequences of the EoS parameters have been

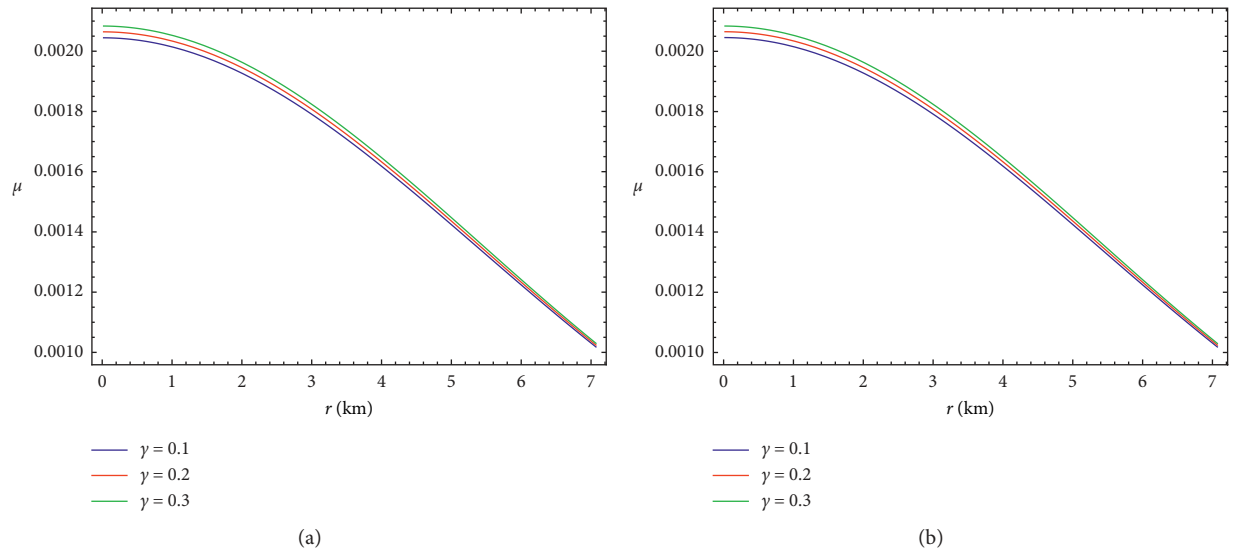


Figure 1: Variation of energy density w.r.t. radial coordinate $r$ of CS1 object for $f(R) = R + \gamma R^2$ (a) and $f(R) = R + \gamma R(R + \alpha R^2)$ (b), by employing $\alpha = 0.5$ in this whole study.

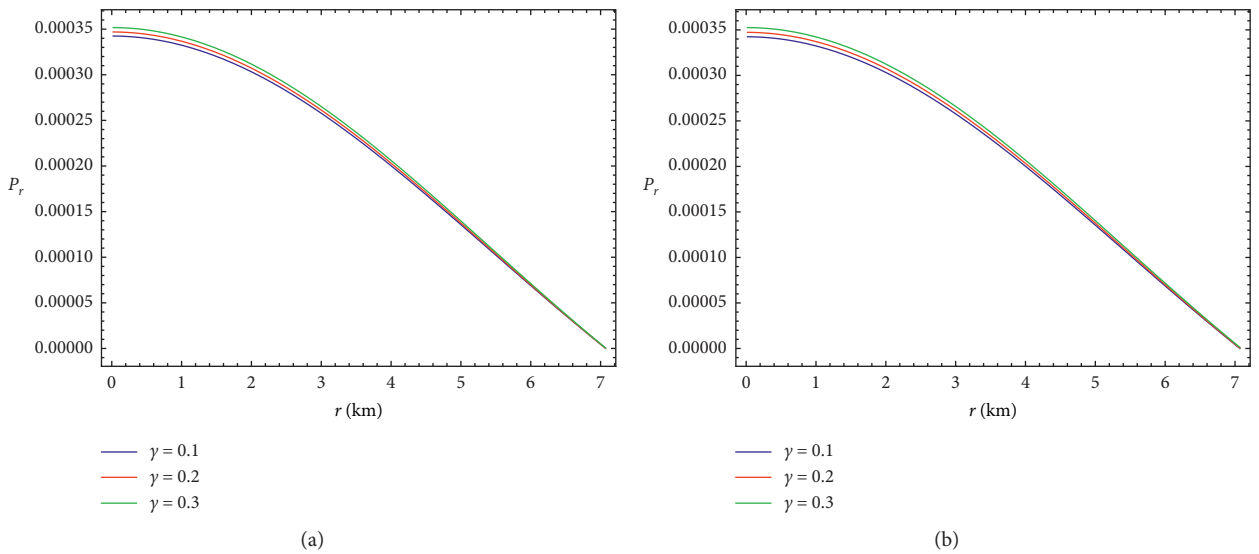


Figure 2: Physical variation of the radial pressure with radial distance $r$ of the CS1 object for two well-known models $f(R) = R + \gamma R^2$ (a) and $f(R) = R + \gamma R(R + \alpha R^2)$ (b).

observed in different mechanisms [115–117]. Thus, the required analytical expressions of EoS parameters for our proposed object are given as

Here $\beta = (\tilde{X} + t\tilde{Y})(2F + rF') - F''$. Figure 6 shows the examination of the physical evolution of EoS parameters, namely, $\omega_r$ and $\omega_t$ for our presented stellar object in the background of two well-known $f(R)$ models. It can be clearly seen from Figure 6 that each combined plot with a magnified image of $\omega_r$ and $\omega_t$ shows positive behavior within the entire configuration of the system and gradually decreases from the center towards the boundary surface of the star. We also note that the nature of $\omega_r$ and $\omega_t$ remains in the range between 0 and (1/3), i.e., $0 < \omega_i < (1/3)$, which clearly signifies the nonexotic behavior [118] of the principal matter configuration.

*5.3. Energy Conditions.* Here, we confirmed various energy conditions for charged anisotropic relativistic strange matter distribution in the framework of metric $f(R)$ gravity. These energy conditions earned a much significant role for any physically realistic choice of interior matter configuration because these must be positive at any interior point of the entire region of the star. Therefore, we satisfied

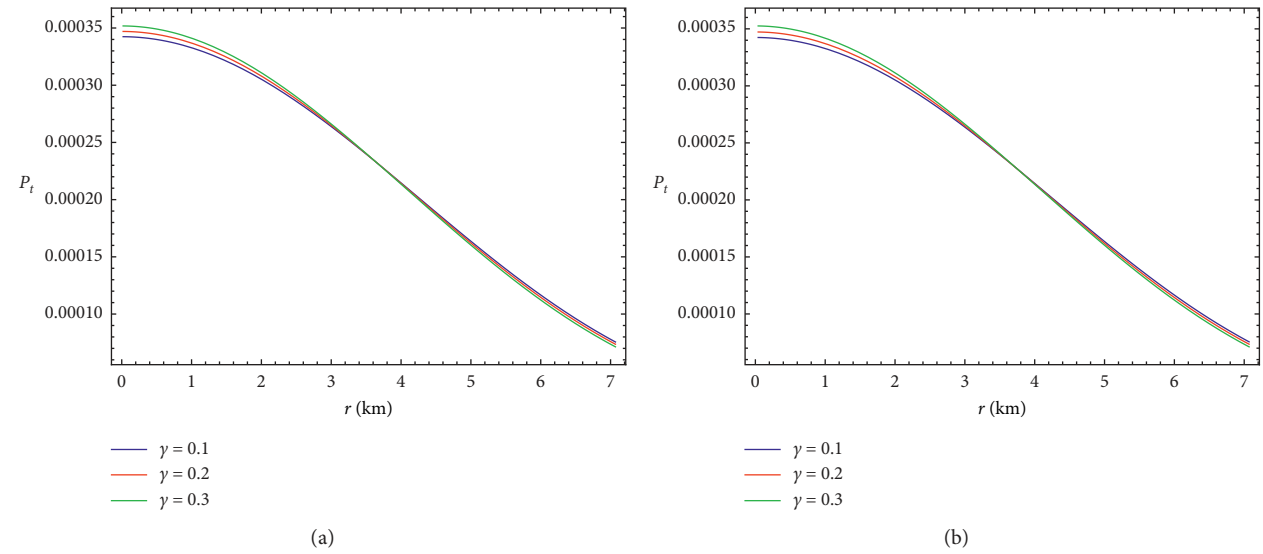


Figure 3: Evolution of transverse pressure $(P_t)$ versus radial coordinate $r$ of the CS1 object with viable models $f(R) = R + \gamma R^2$ (a) and $f(R) = R + \gamma R(R + \alpha R^2)$ (b).

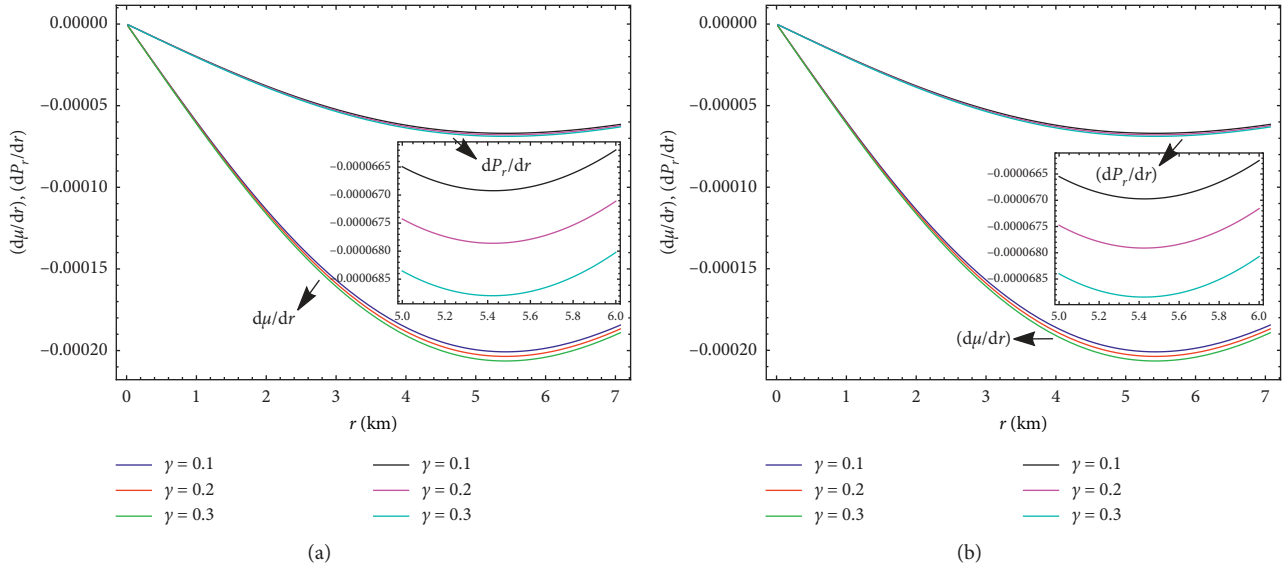


Figure 4: Behavior of $(d\mu/dr)$ and $(dP_r/dr)$ w.r.t. the radial distance $r$ for CS1 candidate for two cosmologically feasible models $f(R) = R + \gamma R^2$ (a) and $f(R) = R + \gamma R(R + \alpha R^2)$ (b).

various energy conditions, namely, null energy conditions (NEC), weak energy conditions (WEC), and strong energy conditions (SEC). The following inequalities fulfill simultaneously for all interior points of the strange star distribution.

$$\text{NEC}: \frac{\mathbb{E}^2}{8\pi} + \mu \geq 0, \tag{27}$$

$$\begin{aligned} &\text{WEC}_r: P_r + \mu \geq 0, \\ &\text{WEC}_t: \frac{\mathbb{E}^2}{4\pi} + P_t + \mu \geq 0, \end{aligned} \tag{28}$$

$$\text{SEC}: \frac{\mathbb{E}^2}{4\pi} + P_r + 2P_t + \mu \geq 0. \tag{29}$$

We determined the combined nature of above inequalities (28)–(30) for our presented strange star candidate with two viable classes of $f(R)$ models in Figure 7. It is obviously seen from Figure 7 that both plots of the combined energy conditions with their respective $f(R)$ models show positive nature within the whole distribution of the star. Thus, the representation tells us that all the energy conditions are satisfied and well tested for our proposed strange star object, which actually indicates towards the physically realistic configuration of the system.

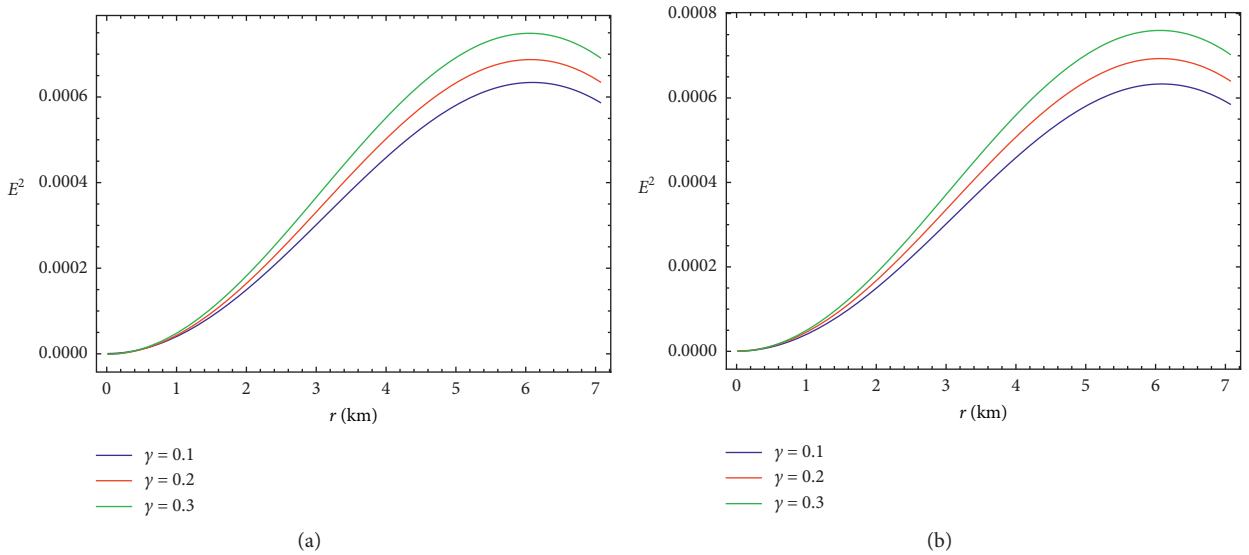


FIGURE 5: Evolution of electric field ($\mathbb{E}^2$) as a function of $r$ for $CS1$ candidate for feasible models $f(R) = R + \gamma R^2$ (a) and $f(R) = R + \gamma R(R + \alpha R^2)$ (b).

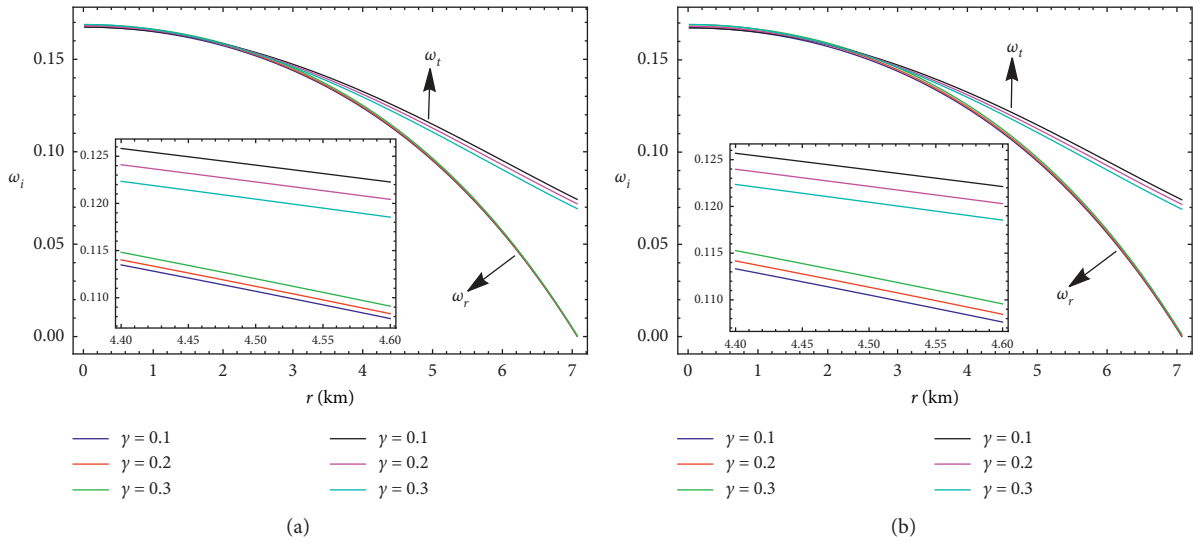


FIGURE 6: Variation of EoS parameters ($\omega_r$ and $\omega_t$) versus $r$ of the CS1 candidate with viable models $f(R) = R + \gamma R^2$ (a) and $f(R) = R + \gamma R(R + \alpha R^2)$ (b).

$$\omega_r(r) = \frac{P_r}{\mu} = \frac{\beta - 32\pi B_g e^{\widetilde{X}r^2}}{3\beta + 32\pi B_g e^{\widetilde{X}r^2}},$$

$$\omega_t(r) = \frac{P_t}{\mu} = \frac{1}{r^2\left(3\beta + 32\pi B_g e^{\widetilde{X}r^2}\right)}\left[12rF' + r^2\left(4(f - RF)e^{\widetilde{X}r^2} - rF'(5\widetilde{X} - 7\widetilde{Y}) + 5F''\right)\right. \tag{30}$$

$$\left. + F\left(4\left(1 - e^{\widetilde{X}r^2}\right) - 2r^2(3\widetilde{X} - 7\widetilde{Y}) - 4r^4\widetilde{Y}(\widetilde{X} - \widetilde{Y})\right) + 32\pi B_g e^{\widetilde{X}r^2}\right].$$

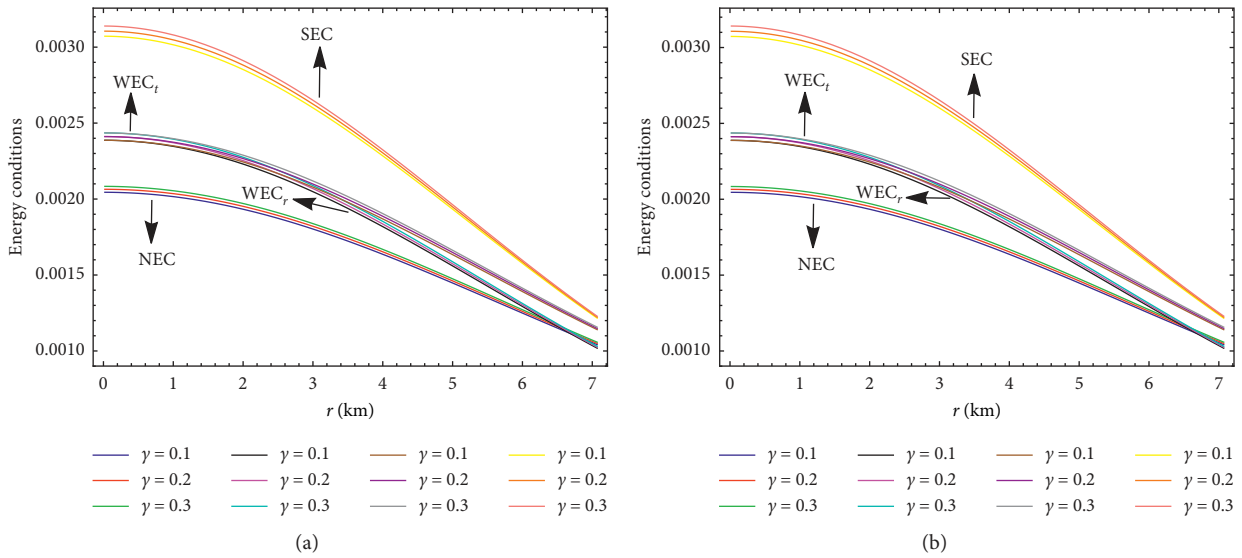


FIGURE 7: The combined behavior of different energy conditions shown against $r$ for CS1 candidate for two well-known models $f(R) = R + \gamma R^2$ (a) and $f(R) = R + \gamma R(R + \alpha R^2)$ (b).

*5.4. Equilibrium Condition.* In this analysis, we focused on the modified hydrostatic equilibrium condition for the investigation of physical viability of our presented strange celestial object. In the modified equilibrium condition, any anisotropic-charged relativistic matter composition is in the stable state under the combined effect of several forces, which are dark force, electric force, anisotropic force, hydrostatic force, and gravitational force. The stable state of any matter composition can be studied by proving the generalized Tolman–Oppenheimer–Volkoff (TOV) equation [119,120,121]. Thus, the modified TOV equation has turned out to be the following form.

$$-(P_r + \mu)\frac{\zeta'}{2} - \frac{dP_r}{dr} + (P_t - P_r)\frac{2}{r} + \frac{e^{(\xi/2)}\rho}{r^2}q - \mathbb{D} = 0, \quad (31)$$

The result of equation (31) defines the stable position for the anisotropic-charged matter sphere under the combined effective behavior of five forces such as dark force ($F_d$) due to $f(R)$ dark source term, electric force ($F_e$), anisotropic force ($F_a$), hydrostatic force ($F_h$), and gravitational force ($F_g$). So, the above result can also provide the following stable formation:

$$F_g + F_h + F_a + F_e + F_d = 0, \quad (32)$$

where

$$\begin{aligned} F_g &= -(P_r + \mu)\tilde{Y}r, \\ F_h &= -\frac{dP_r}{dr}, \\ F_a &= (P_t - P_r)\frac{2}{r}, \\ F_e &= \rho e^{\left(\tilde{X}r^2/2\right)}\mathbb{E}, \\ F_d &= -\mathbb{D}. \end{aligned} \quad (33)$$

Here, $\mathbb{D}$ represents the dark source term determines from the fourth order $f(R)$ geometry and is given by

$$\begin{aligned} \mathbb{D} = \frac{1}{8\pi}\Bigg[&\left\{e^{-\tilde{X}r^2}\left(-\frac{1}{2}(f - RF) - F'e^{-\tilde{X}r^2}\left(r\tilde{Y} + \frac{2}{r}\right)\right)\right\}' + \frac{\tilde{Y}r}{e^{2\tilde{X}r^2}}\{F'' - (\tilde{X} + \tilde{Y})rF'\} \\ &+ \frac{2\tilde{X}r}{e^{\tilde{X}r^2}}\left\{-\frac{1}{2}(f - RF) - F'e^{-\tilde{X}r^2}\left(\tilde{Y}r + \frac{2}{r}\right)\right\} + \frac{2}{re^{2\tilde{X}r^2}}\left\{F'' - \left(\tilde{X}r + \frac{1}{r}\right)F'\right\}\Bigg]. \end{aligned} \quad (34)$$

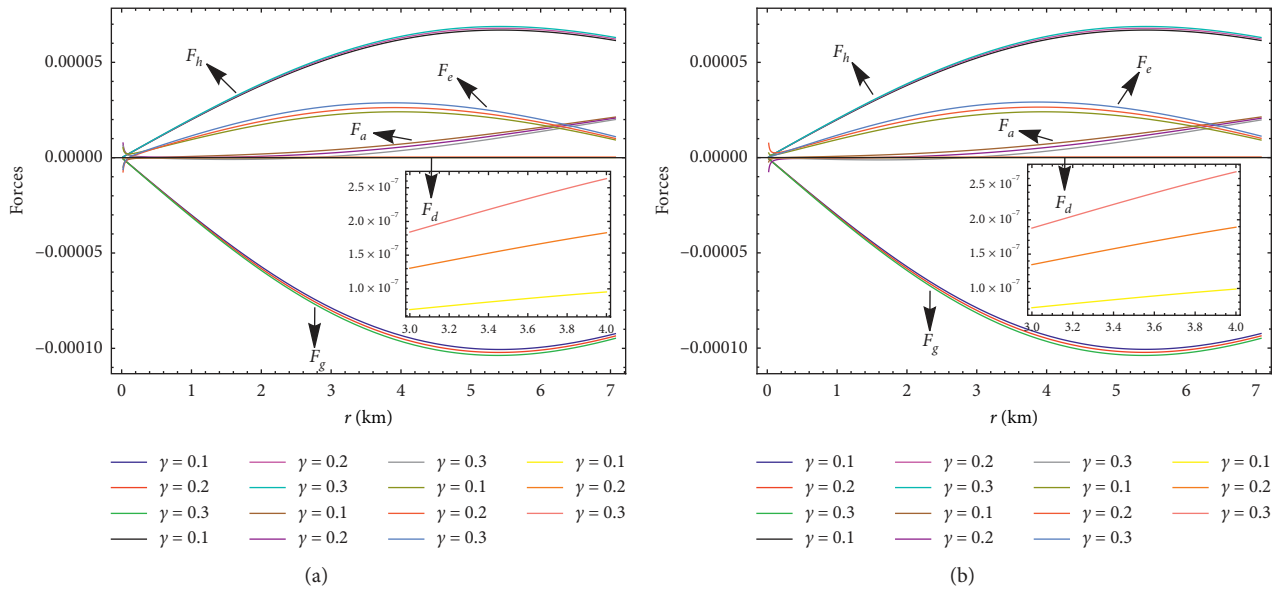


FIGURE 8: The combined nature of five distinct forces has been plotted versus radial distance $r$ for the CS1 object for two well-known models $f(R) = R + \gamma R^2$ (a) and $f(R) = R + \gamma R(R + \alpha R^2)$ (b).

We plot the combined action of five different forces predicted by equation (32) for the presented CS1 object with two different choices of viable $f(R)$ models as shown in Figure 8. One can easily note from Figure 8 that each plot of the equilibrium condition with their respective $f(R)$ models suggests that the hydrostatic, anisotropic, electric, and dark forces act in outward direction or have a repulsive role in nature and gravitational force acts in inward direction or have an attractive role in nature. As a result, we can say that our present strange star candidate is in better equilibrium situation and a physically more reliable candidate.

*5.5. Anisotropy Estimation.* We examined the anisotropic stress for our obtained solutions of the stellar system in the background of two specific $f(R)$ models. The anisotropy of the present strange star object can be defined as

$$\Delta = P_t - P_r = \frac{1}{8\pi}\left[\left\{\left(3\widetilde{Y} - 2\widetilde{X} - \widetilde{X}\widetilde{Y}r^2 + \widetilde{Y}^2r^2 + \frac{1}{r^2}\right)e^{-\widetilde{X}r^2} - \frac{1}{r^2}\right\}F + \left\{(f - RF) + e^{-\widetilde{X}r^2}\left(\left(\frac{3\widetilde{Y}r}{2} - \frac{3\widetilde{X}r}{2} + \frac{3}{r}\right)F' + \frac{3F''}{2}\right)\right\}\right] + 2B_g. \tag{35}$$

Equation (35) describes the effect of anisotropic force $(2(P_t - P_r)/r)$ on the charged spherical system that generates due to the anisotropic stress of the source. If the pressure anisotropy acts in outward direction or will be repulsive in nature, then $\Delta > 0$, i.e., $P_r < P_t$, whereas if it acts inward direction or attractive in nature, then $\Delta < 0$, i.e., $P_r > P_t$, as predicted by Hossein et al. [77]. Figure 9 shows the graphical nature of anisotropic stress of the fluid sphere by using two well-known $f(R)$ models. It is obviously seen from Figure 9 that the anisotropic pressure gradually boosts from the center towards the boundary surface of the star where $r = \widetilde{x}$, and it remains positive throughout the whole configuration of the sphere or $P_t - P_r > 0$. This constraint yields that the pressure anisotropy is in outward direction or repulsive in nature, and it helps to construct the ultradense compact stellar body [122, 123].

*5.6. Stability Analysis.* We investigated the stability via Herrera's causality condition and the cracking method [124, 125] for the physical acceptability of the presented solutions by employing different unknown parameter values. The causality condition of the stability analysis tells us that the square of the radial sound speed $\nu_{rs}^2$ and the transverse sound speed $\nu_{ts}^2$ should always remain in the range between $0 \le \nu_{rs}^2 \le 1$ and $0 \le \nu_{ts}^2 \le 1$. Another method describes that the region for which the radial sound speed exceeds than that of tangential sound speed is a potentially stable region [124–128]. As a result, Herrera [125], Abreu et al. [127], and Andréasson [128] suggest the inequality $|\nu_{ts}^2 - \nu_{rs}^2| \le 1$ for stable matter configuration. This inequality is familiarized as "no cracking" to occur, i.e., potentially stable region. The generic formulae of the squares of radial and tangential sound speeds can be written as

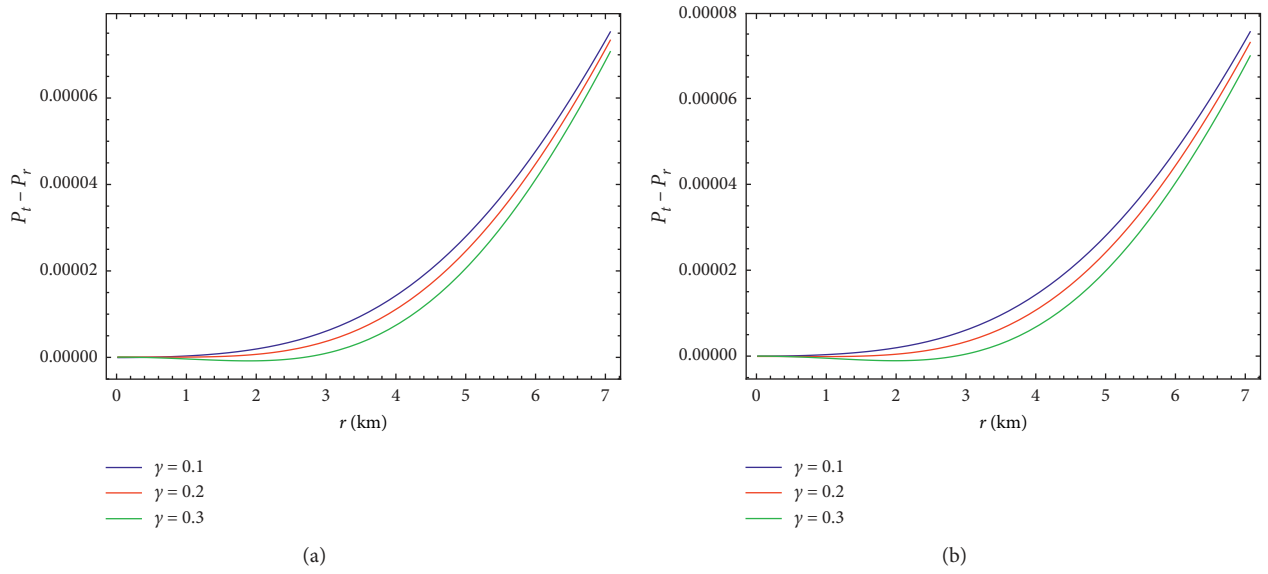


FIGURE 9: Physical evolution of the anisotropy w.r.t. radial coordinate $r$ for the CS1 object for $f(R) = R + \gamma R^2$ (a) and $f(R) = R + \gamma R(R + \alpha R^2)$ (b) models.

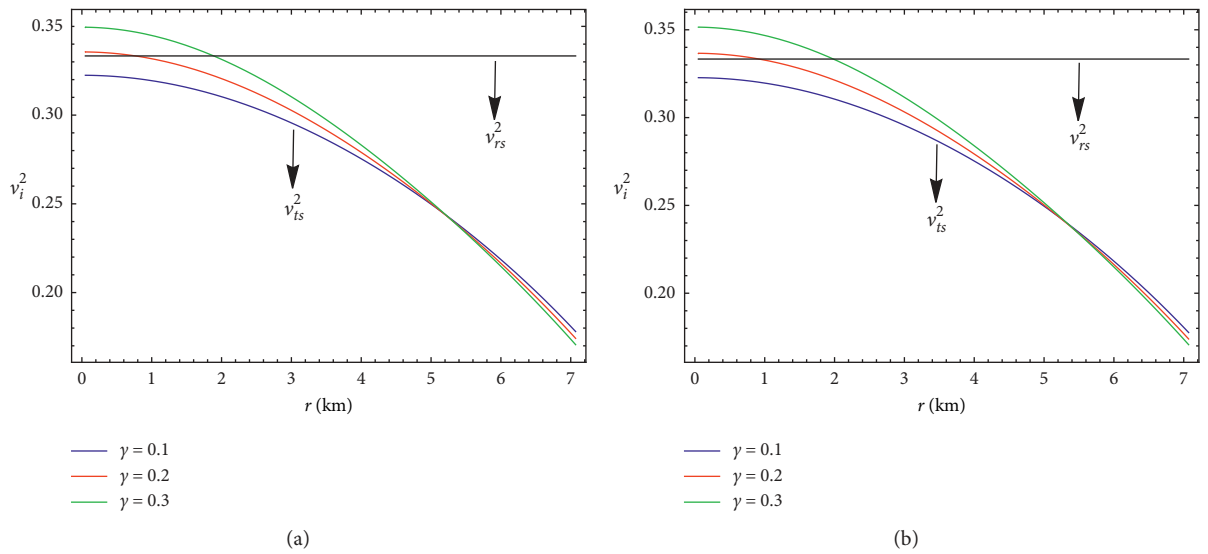


FIGURE 10: The sound speeds $v_r^2$ and $v_t^2$ with radial distance $r$ are represented according to equations (36) and (37) for the candidate CS1 for $f(R) = R + \gamma R^2$ (a) and $f(R) = R + \gamma R(R + \alpha R^2)$ (b) models.

$$v_{\mathrm{rs}}^2 = \frac{dP_r}{d\mu} = \frac{1}{3}, \tag{36}$$

$$v_{\mathrm{ts}}^2 = \frac{dP_t}{d\mu}. \tag{37}$$

Figure 10 explains the nature of the causality condition for the proposed CS1 object w.r.t. two well consistent $f(R)$ models. The profile of the causality condition shows that the squares of radial and tangential sound speeds does not cross the certain range $0 \le v_i^2 \le 1$ within the whole distribution of the star. From Figure 11, we determine the potential stable configuration for the inequality $v_{\mathrm{ts}}^2 - v_{\mathrm{rs}}^2 < 0$. This inequality suggests that "no cracking" occurs within a fluid sphere, which indicates the confirmation of Herrera's cracking concept [125]. The magnitude of the difference between the squares of tangential and radial sound speeds is shown in Figure 12. It can be easily understood from Figure 12 that each plot of $|v_{\mathrm{ts}}^2 - v_{\mathrm{rs}}^2| \le 1$ with their respective $f(R)$ models represents the monotonically increasing nature with the

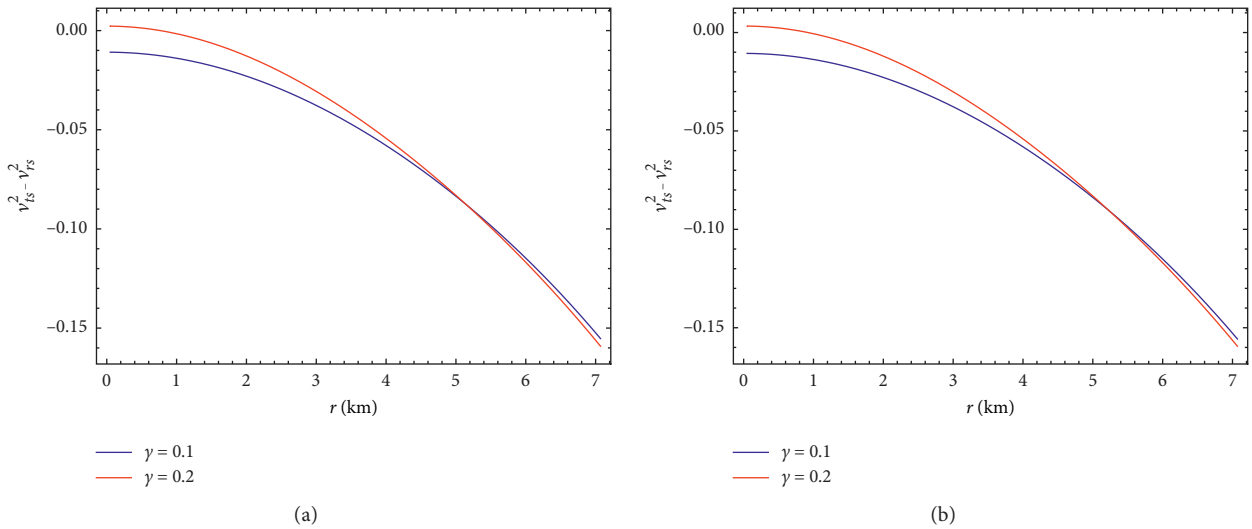


Figure 11: Evolution of $v_{ts}^2 - v_{rs}^2$ vs. $r$ of the CS1 candidate for $f(R) = R + \gamma R^2$ (a) and $f(R) = R + \gamma R(R + \alpha R^2)$ (b) models.

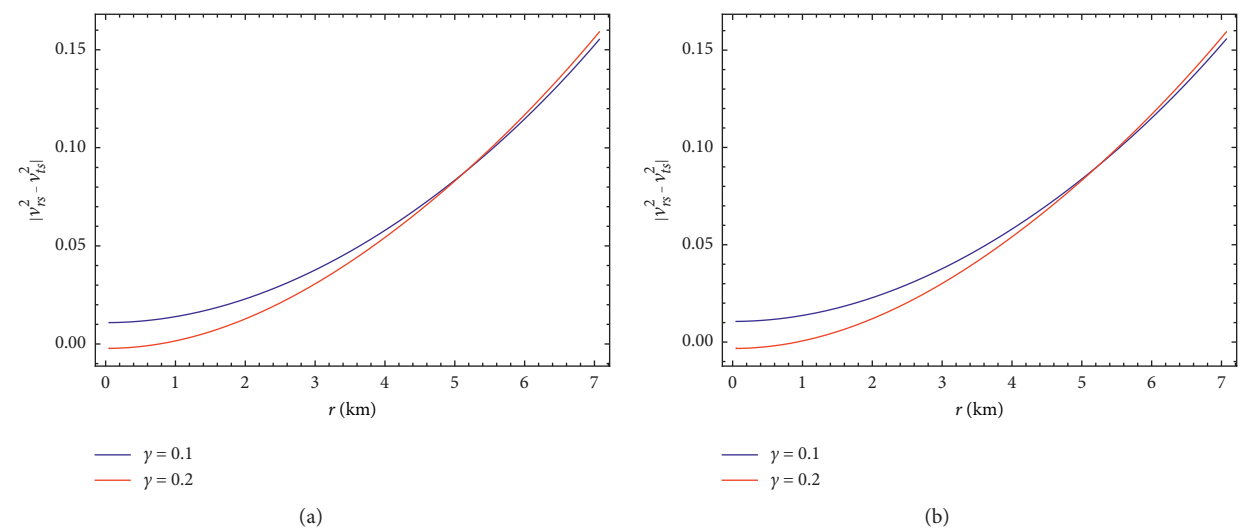


Figure 12: Physical behavior of $|v_{ts}^2 - v_{rs}^2|$ has been drawn against $r$ for the object CS1 with $f(R) = R + \gamma R^2$ (a) and $f(R) = R + \gamma R(R + \alpha R^2)$ (b) models.

increase of $r$, but it always less than one. Consequently, our present system maintains the stability with Herrera's cracking method and resumes the stable position.

*5.7. Static Stability Criterion.* Another important criterion is the static stability to study the stable position of the compact celestial object. This criterion was considered by Harrison et al. [129] and Zel' dovich–Novikov [130] for stable equilibrium position of the matter object. They proposed that the matter of the celestial body should be the boosting function w.r.t. of the central density for the stable equilibrium position, i.e., $(dM/d\mu(0)) > 0$, and it will be the unstable position in case of $(dM/d\mu(0)) < 0$. For our proposed candidate, the mass in terms of central density is defined as

$$M(\mu(0)) = -e^{\left[\ln(\tilde{x}/2) - \tilde{x}^2\left\{(8\pi\mu(0)/3F) + (1/F)\left((1/6)(f - RF) + F''\right)\right\}\right]} + \frac{Q^2}{2\tilde{x}} + \frac{\tilde{x}}{2}. \tag{38}$$

Alternatively, we obtain

$$\frac{dM}{d\mu(0)} = \frac{8\pi\tilde{x}^2}{3F} e^{\left[\ln(\tilde{x}/2) - \tilde{x}^2\left\{(8\pi\mu(0)/3F) + (1/F)\left((1/6)(f - RF) + F''\right)\right\}\right]}. \tag{39}$$

We plot the graphical evolution of mass as a function of central density for CS1 candidate with their respective

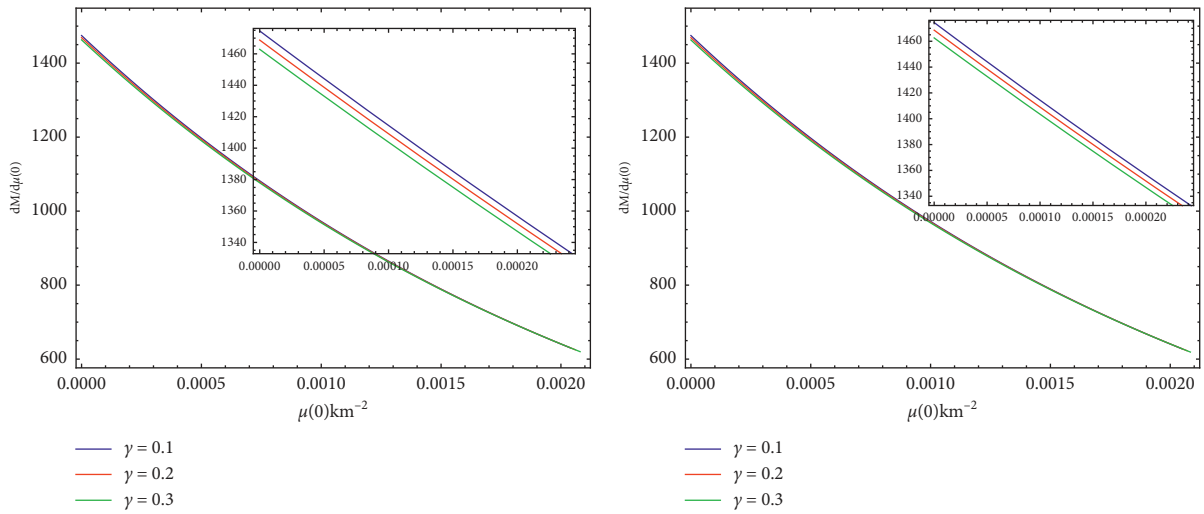


FIGURE 13: The nature of $(\mathrm{d}M/\mathrm{d}\mu(0))$ shown vs. central density $(\mu(0))$ for the object CS1 for viable models $f(R) = R + \gamma R^2$ (a) and $f(R) = R + \gamma R(R + \alpha R^2)$ (b).

models of $f(R)$ (Figure 13). Each profile of $(\mathrm{d}M/\mathrm{d}\mu(0))$ with a magnified image represents the positive evolution in the entire region of the star, and it attains the maximum amount at the center of the sphere. Accordingly, there is another condition that confirms the stability position for our stellar system.

*5.8. Adiabatic Index.* The term adiabatic index is described as the ratio of two specific heats [131]. The adiabatic index is the foremost parameter that ruins the stability of any celestial body. We can employ it to examine the stability of relativistic and nonrelativistic source systems. For anisotropic source distribution, the Bondi [132] analysis reveals that the adiabatic index $\Gamma$ can be written as radial and transverse adiabatic indices $\Gamma_r$ and $\Gamma_t$, respectively. According to Bondi [132], for the stable Newtonian system, $\Gamma_r > (4/3)$ and $\Gamma_r = (4/3)$ are the constraints of neutral equilibrium. For the relativistic isotropic system, the above constraint changes due to the regenerative effect of the pressure which manifests the system more unstable. In case of the general relativistic anisotropic system, more problems emerge because the nature of anisotropy determines the stability of the celestial body. The adiabatic index must be greater than $(4/3)$ in an interior relativistic anisotropic stable star as proposed by several researchers [131, 133, 134]. Thus, the adiabatic indices ($\Gamma_r$ and $\Gamma_t$) for our obtained solutions are expressed as

$$\Gamma_r = \left(\frac{\mu + P_r}{P_r}\right)\frac{\mathrm{d}P_r}{\mathrm{d}\mu}, \tag{40}$$

$$\Gamma_t = \left(\frac{\mu + P_t}{P_t}\right)\frac{\mathrm{d}P_t}{\mathrm{d}\mu}. \tag{41}$$

The evolutionary nature of both adiabatic indexes ($\Gamma_r$ and $\Gamma_t$) in Figures 14 and 15 indicate the viability of our presented CS1 object w.r.t. two specific $f(R)$ models. One can eminently observe that from Figures 14 and 15, both the profiles of adiabatic indices show monotonically increasing nature with the increase of $r$ and remain positive in the whole configuration of the star. It would be necessary to mention here that $\Gamma_r$ and $\Gamma_t$ exceed than $(4/3)$ within the entire region of the celestial sphere, which signifies the potentially stable position of the CS1 object against the radial perturbation.

## 6. Effective Mass Function, Compactification Factor, and Surface Redshift

In this evaluation, we studied the effective gravitational mass function as well as other standard prominent profiles for the physical credibility of our proposed compact celestial object in the presence of two viable $f(R)$ models. Thus, we initially discuss the modified effective gravitational mass function for the charged anisotropic source distribution as reported by equation (7) which reads

$$M_{\mathrm{eff}} = 4\pi\int_0^r \frac{1}{F}\left(\frac{\mathbb{E}^2}{8\pi} + \mu\right)r^2\mathrm{d}r = \frac{r}{2}\left(1 - e^{-\widetilde{\mathrm{X}}r^2}\right) - \frac{1}{2}\int_0^r \frac{r^2}{F}\left[\frac{1}{2}(f - \mathrm{RF}) + e^{-\widetilde{\mathrm{X}}r^2}\left(F'' + \left(\frac{2}{r} - \widetilde{\mathrm{X}}r\right)F'\right)\right]\mathrm{d}r. \tag{42}$$

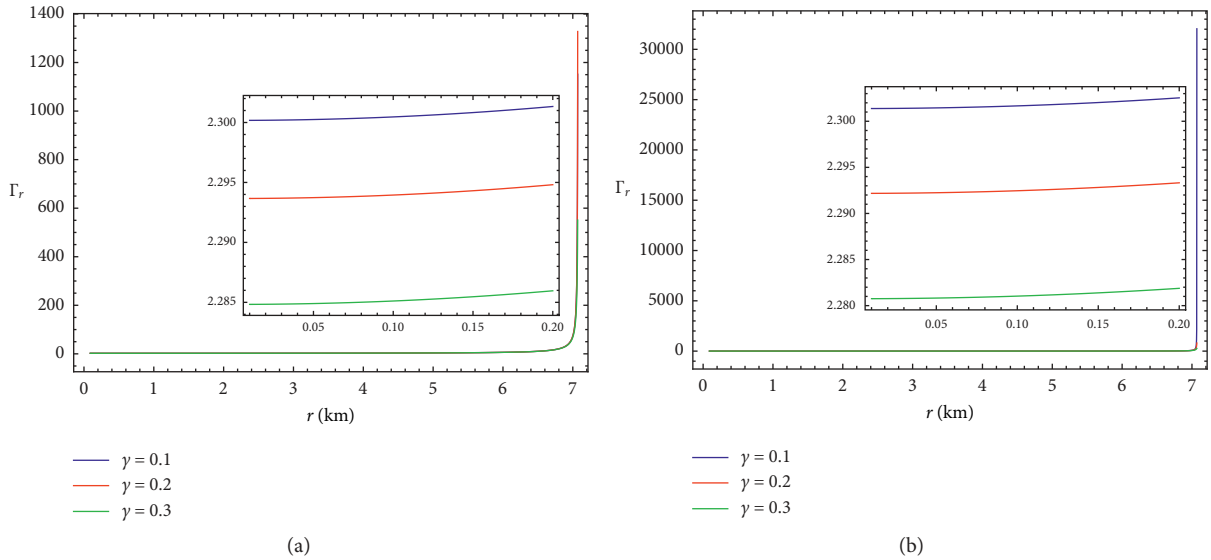


FIGURE 14: The adiabatic index $(\Gamma_r)$ with the radial coordinate $r$ plotted according to equation (40) for the CS1 candidate for feasible models $f(R) = R + \gamma R^2$ (a) and $f(R) = R + \gamma R(R + \alpha R^2)$ (b).

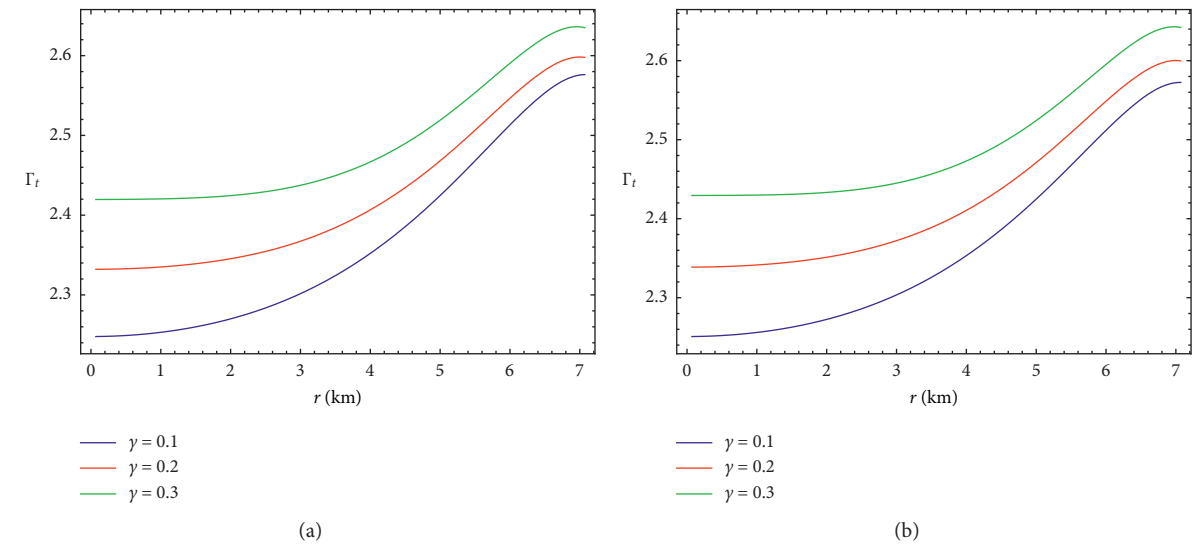


FIGURE 15: The adiabatic index $(\Gamma_t)$ versus $r$ has been drawn according to equation (41) for the CS1 candidate for two well-known models $f(R) = R + \gamma R^2$ (a) and $f(R) = R + \gamma R(R + \alpha R^2)$ (b).

The physical determination of effective gravitational mass for the CS1 candidate in the presence of two specific $f(R)$ models is shown in Figure 16. It is clearly seen from Figure 16 that each plot of effective gravitational mass indicates that the evolution is positive throughout the interior distribution of the star and is a monotonically increasing function of the radial parameter $r$. It is also noticed here that the mass function is regular at the center of the star, i.e., $r \longrightarrow 0$ and $M_{\text{eff}} \longrightarrow 0$. Besides this picture, one vital point to mention here is that the maximal numerical value in each profile remains in the limit 2.1166 (Table 7). Hence, this result strongly suggests that our proposed strange star candidate is physically acceptable and well consistent.

According to Buchdahl [135], for static isotropic fluid sphere, the maximum allowable limit of twice the mass to radius ratio of a compact object should be less than (8/9), i.e., $(2M/\widetilde{x}) < (8/9)$. Later, this result was generalized by Mak et al. [136] for the charged relativistic source distributions. In 2009, Andreeasson [128] generalized Buchdahl's result for relativistic charged anisotropic matter configuration and formulated the upper bound on the mass to radius ratio for the charged spherical system as $M \leq ((\sqrt{R}/3) + \sqrt{(R/9) + (Q^2/3R)})^2$. To derive this solution, Andreeasson considered the relation between pressures ($P_r$ and $P_t$) and energy density as $P_r - \mu + 2P_t \leq 0$. This condition must be fulfilled for the allowable limit of

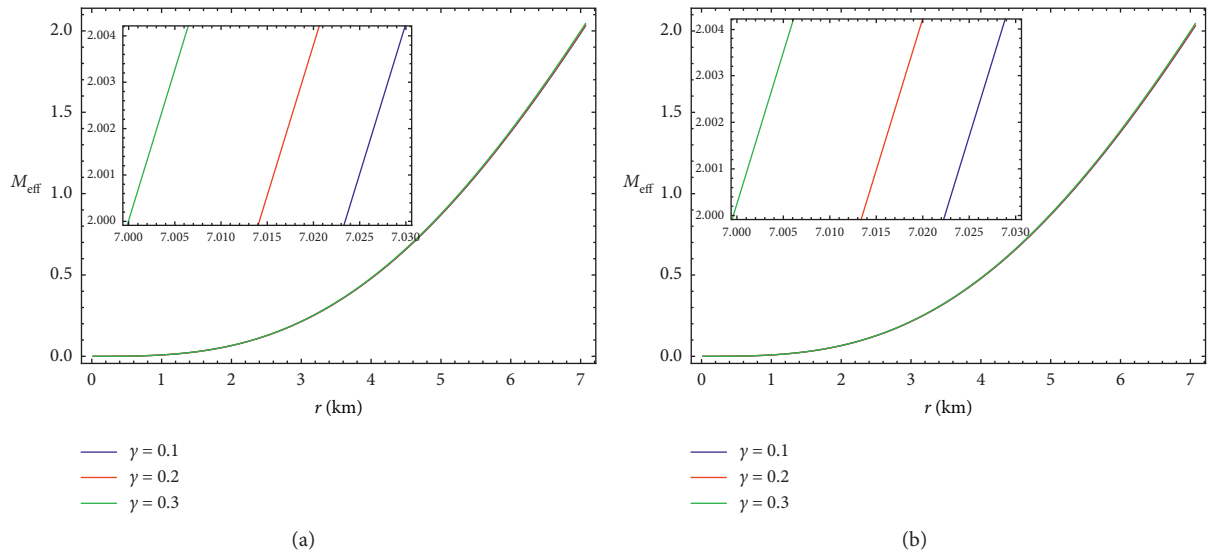


FIGURE 16: Profile of the effective mass function as a function of $r$ for CS1 candidate for models $f(R) = R + \gamma R^2$ (a) and $f(R) = R + \gamma R(R + \alpha R^2)$ (b).

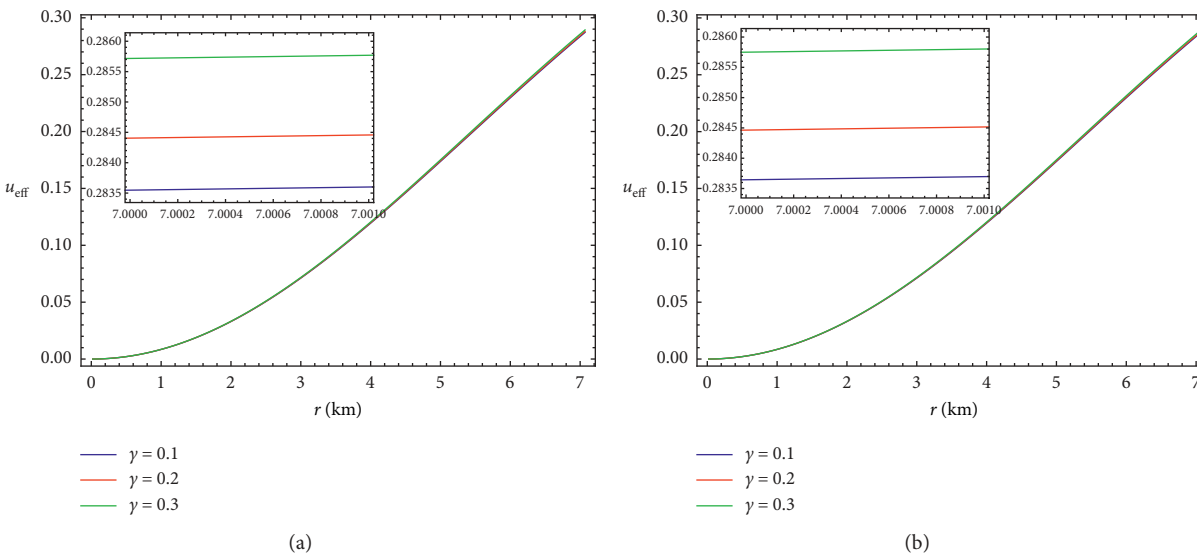


FIGURE 17: Physical evolution of compactness vs. $r$ of the CS1 object with viable models $f(R) = R + \gamma R^2$ (a) and $f(R) = R + \gamma R(R + \alpha R^2)$ (b).

Andŕeasson. So, the required compactification factor of the stellar star is as follows:

$$u_{\text{eff}} = \frac{M_{\text{eff}}}{r} = \frac{1}{2}\left(1 - e^{-\widetilde{X}r^2}\right) - \frac{1}{2r}\int_0^r \frac{r^2}{F}\left[\frac{1}{2}(f - \text{RF}) + e^{-\widetilde{X}r^2}\left(F'' + \left(\frac{2}{r} - \widetilde{X}r\right)F'\right)\right]\text{dr}. \tag{43}$$

Figure 17 illustrates the compactification factor against the radial coordinate $r$ for the present stellar configuration with two prominent types of $f(R)$ models. Each plot transparently shows that the compactification increases with the increase of $r$ and attains the maximum position at the boundary surface of the star. Moreover, this maximum position of $(M/\widetilde{x})$ always remain in the specified range of Buchdahl [135]. We analyzed the evolution of Andŕeasson inequality $P_r - \mu + 2P_t$ w.r.t. radial parameter $r$ (Figure 18). One can easily observe from Figure 18 that both profiles of $P_r - \mu + 2P_t$ represent the

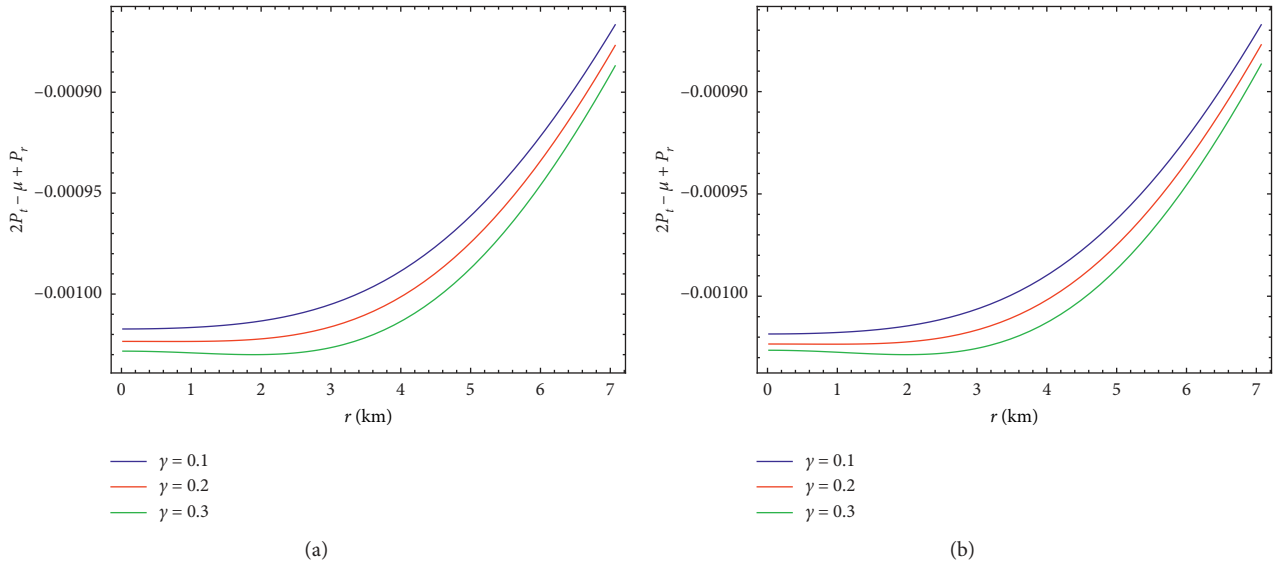


FIGURE 18: Physical evolution of $P_r - \mu + 2P_t$ vs. $r$ of the CS1 object with viable models $f(R) = R + \gamma R^2$ (a) and $f(R) = R + \gamma R(R + \alpha R^2)$ (b).

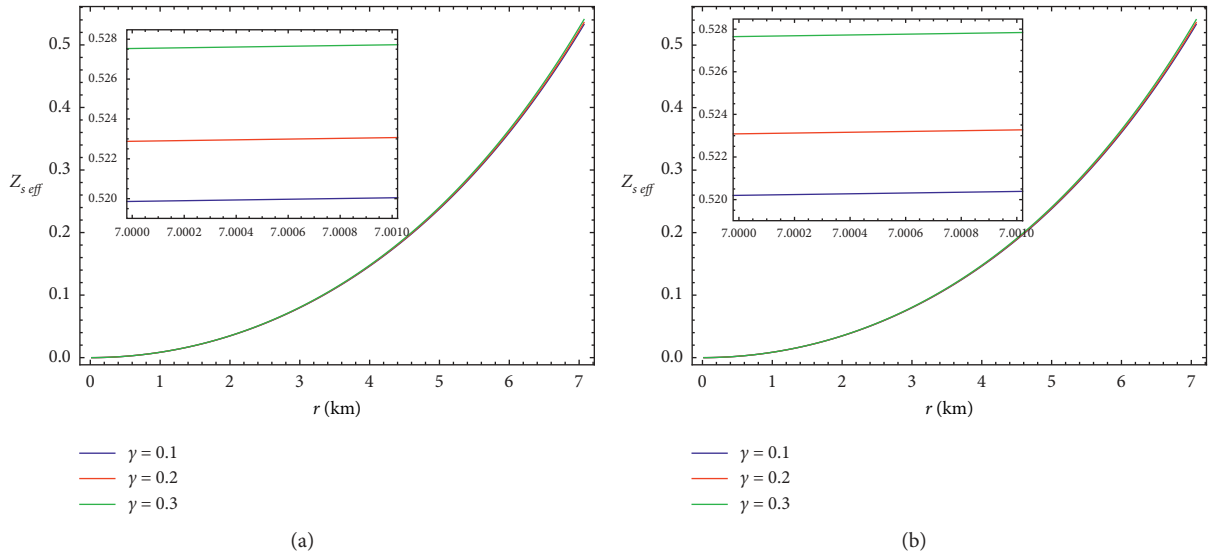


FIGURE 19: The surface redshift w.r.t. radial coordinate $r$ represented according to equation (44) for the CS1 candidate for feasible models $f(R) = R + \gamma R^2$ (a) and $f(R) = R + \gamma R(R + \alpha R^2)$ (b).

negative evolution at every interior point of the fluid sphere that actually confirms Andreeasson bound. Hence, these results evidently suggest that our considered celestial object should be a strange star candidate.

The surface redshift corresponding to the compactification factor can be defined as

$$Z_s = \frac{1}{\left(1 - 2u_{\text{eff}}\right)^{(1/2)}} - 1 = \left[1 - \left(1 - e^{-\widetilde{X}r^2}\right) + \frac{1}{r}\int_0^r \frac{r^2}{F}\left[\frac{1}{2}(f - RF) + e^{-\widetilde{X}r^2}\left(F'' + \left(\frac{2}{r} - \widetilde{X}r\right)F''\right)\right]\mathrm{dr}\right]^{(-1/2)} - 1. \tag{44}$$

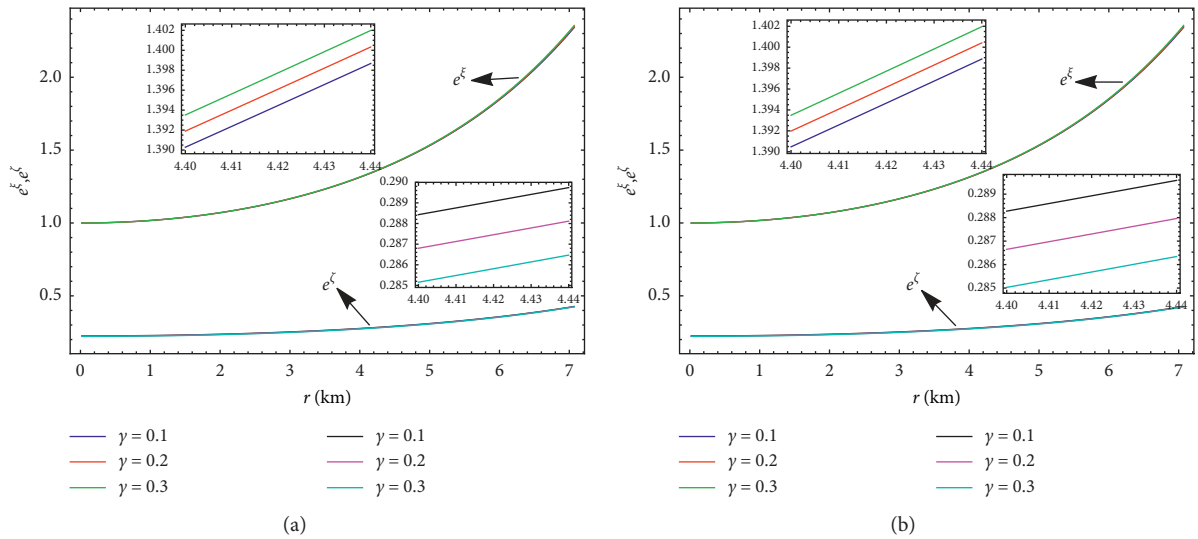


Figure 20: Combined graphical behaviors with magnified images of the metric potentials ($e^{\xi(r)}$ and $e^{\zeta(r)}$) versus $r$ for compact object (CS1) SAX J 1808.4-3658 with their respective unknown arbitrary constant values given in Tables 1 and 2 for two viable models $f(R) = R + \gamma R^2$ (a) and $f(R) = R + \gamma R(R + \alpha R^2)$ (b). From each plot of the metric potentials, the evolution is positive throughout the interior compact object and attains maximum position towards the boundary surface.

Here, we report some novel results of surface redshift upper bound for isotropic and anisotropic matter distributions with and without a cosmological constant. Barraco and Hamity [137] investigated $Z_s \leq 2$ for isotropic fluid sphere in the absence of a cosmological constant, whereas Ivanov [138] proved that the maximum allowable value of surface redshift must lie in the range $Z_s = 3.842$ for the isotropic star. In the presence of a cosmological constant, Bohmer and Harko [139] calculated the maximum upper bound of surface redshift as $Z_s \leq 5$ for anisotropic fluid sphere. In connection of this discussion, for anisotropic-charged strange star models, the maximum value of surface redshift is in better position for our present CS1 candidate. We plot the graphical behavior of surface redshift as a function of $r$ for the present stellar star candidate w.r.t. two viable $f(R)$ models (Figure 19). It can be clearly seen from Figure 19 that both profiles of surface redshift show monotonically increasing nature throughout the interior star distribution, and it is finite at the center of the sphere where $r = \tilde{x} = 0$. So, this position ultimately indicates that our strange star models are in good agreement and physically well consistent (Figure 20).

## 7. Conclusions

The present manuscript explored the new viable solutions of charged anisotropic strange star models by implementing the observational values of well-known compact objects within the framework of so-called $f(R)$ theory of gravity. This investigation was made for relativistic charged fluid sphere case in the assistance of the simple MIT bag model EoS and KB type metric solutions $\zeta(r) = \tilde{Y}r^2 + \tilde{Z}$ and $\xi(r) = \tilde{X}r^2$ [96]. The results of this technique for our compact star candidates are free from central singularity as well as physically acceptable with two well-known and cosmologically viable $f(R)$ models such as $f(R) = R + \gamma R^2$ [102] and $f(R) = R + \gamma R(R + \alpha R^2)$ [42] at the theoretical and the astrophysical gauge. For this evaluation, from the set of equations (7)–(11) along with KB type metric solutions, we have found out the solutions of different physical parameters for the graphical nature of our proposed compact object. Thereafter, we have determined unknown arbitrary constant values by employing the smooth matching between the interior and exterior Reissner–Nordström spacetimes at the bounding three-surface. Moreover, the numerical values of these unknown arbitrary constants, central parameters ($\mu(0)$ and $P_r(0)$), and surface parameter ($\mu(\tilde{x})$) for distinct intervals of free parameter $\gamma$ of two viable $f(R)$ models $f(R) = R + \gamma R^2$ and $f(R) = R + \gamma R(R + \alpha R^2)$ against three distinct compact celestial objects ((CS1)SAXJ1808.4 − 3658 ($\tilde{x} = 7.07$ km), (CS2)Vela$X-1$ ($\tilde{x} = 9.56$ km), and (CS3)$4U1820-30$ ($\tilde{x} = 10$ km)) are given in Tables 1–6. Accordingly, we have mentioned several important silent features for our proposed CS1 candidate in the following way:

(i) Metric coefficients: the metric coefficients or metric potentials are geometrical representatives of the spacetime, and it is also independent from physical and geometrical singularities. Their evolution in both $f(R)$ models for CS1 candidate represents positive nature within the entire region of the star and gradually increases with the increase of the radial parameter $r$ (Figure 20).

(ii) Density, pressure, and electric field: we plotted the evolution of several physical parameters, namely, energy density, radial and tangential pressures, electric field, and derivative function of energy density and radial pressure w.r.t. two particular types of $f(R)$ models in Figures 1–5, respectively. One can easily observe from Figures 2–5 that each

profile of energy density, radial pressure, tangential pressure, and electric field suggests positive evolution throughout the whole interior distribution of the fluid sphere and remains regular (finite) at every interior point of the star. One important point that should be necessarily discussed is that the numerical values of central density are greater than the surface density (Tables 1–6), which actually expected the very massive strange quark star objects [107–110]. We have also noted that the radial pressure sharply dies out at the boundary surface of the sphere, but tangential pressure does not exactly vanish, which clearly signifies the spheroidal nature for our CS1 candidate [112–114]. We have observed that from the evolutionary behavior of electric field, it remains positive and finite at every point of the interior compact sphere. Next, we investigated the combined graphical nature of derivative function of energy density and radial pressure as shown in Figure 4. The nature of both profiles with their respective models remains nonpositive within the whole distribution of the compact star and disappears at the core, which strongly supports the maximum rate of energy density and radial pressure for our presented model.

(iii) Energy conditions: we shed light over different energy conditions such as null energy conditions (NEC), weak energy conditions (WEC), and strong energy conditions (SEC) for the physical viability of our obtained solutions. These energy conditions have been satisfied at every interior point of the fluid sphere and always remain positive in the entire region of the star (Figure 7).

(iv) Hydrostatic equilibrium equation: there is another important feasible criterion that has been fulfilled by the modified conservation equation or generalized TOV equation (31) as predicted by under the action of five different forces, namely, additional dark force ($F_d$), electric force ($F_e$), anisotropic force ($F_a$), hydrostatic force ($F_h$), and gravitational force ($F_g$). We examined the combined graphical nature of five forces with their respective $f(R)$ models for our proposed compact star candidate as shown in Figure 8. The combined effect of dark force, electric force, anisotropic force, and hydrostatic force balanced the effect of gravitational force. So, the presented situation has satisfied the equilibrium position [120, 121] for our CS1 object. The modified TOV equation (31) can be reproduced into the standard GR form by simply imposing $f(R) = R$.

(v) Anisotropy: in our proposed star candidate, the anisotropy of pressure maintains positive nature, i.e., $P_t - P_r > 0$ within the entire region of the star, and it is regular (singularity free) at the core of the fluid sphere (Figure 9). Moreover, it monotonically increases from the center towards the boundary surface of the star and attains maximum limit. This maximum limit tells us that our proposed compact object predicted an ultradense strange quark star [123].

(vi) Stability analysis: we checked the stability condition by employing Herrera's causality condition and the cracking method [124, 125] for our physically acceptable solutions (Figures 10–12). The inequalities $0 \le \nu_{rs}^2 \le 1$, $0 \le \nu_{ts}^2 \le 1$, $\nu_{ts}^2 - \nu_{rs}^2 < 0$, and $|\nu_{ts}^2 - \nu_{rs}^2| < 1$ have been satisfied inside the compact celestial object and always remain in the certain range throughout the whole distribution of the sphere (Figures 10–12). Therefore, the presented position strongly defends that our proposed object is in good situation or physically in a potential stable state [124–128].

(vii) Static stability criterion: Harrison-Zel' dovich–Novikov criterion of static stability [129, 130] was estimated (Figure 13) for CS1 candidate. We observed from Figure 13 that the physical evolution of mass function w.r.t. central density $\mu(0)$ remains nonnegative in the entire configuration of the star, i.e., $(\mathrm{d}M/\mathrm{d}\mu(0)) > 0$. Consequently, our presented stellar system obeys the stability condition by the Harrison-Zel 'dovich–Novikov approach.

(viii) Adiabatic indices: the adiabatic indices $\Gamma_r$ and $\Gamma_t$ were graphically analyzed for our presented object with two specific viable $f(R)$ models, respectively (Figures 14 and 15). Each plot of adiabatic indices with their respective profiles suggests the positive nature in the whole interior distribution of the star, and it is a monotonically increasing function of the radial coordinate $r$. Moreover, it is finite at every interior point of the sphere and also greater than $(4/3)$ at the core of the star, which actually indicates the stable Newtonian position for our star [132].

(ix) Equation of state: we have proved another stability criterion by using EoS parameters for our physically realistic solutions. From Figure 6, we have observed that the variation of EoS parameters ($\omega_r$ and $\omega_t$) always remains in the range between 0 and $(1/3)$. It transparently shows that $\omega_r$ and $\omega_t$ are nonnegative within the entire region of the sphere and attain maximum amount at the core of the star where ($r = \tilde{x} = 0$) and gradually decreases with the increase of radial parameter $r$. Indeed, as a result, the matter configuration is nonexotic in nature [118].

(x) Mass function, compactification factor, and surface redshift: the physical variation of different profiles such as mass function, compactification factor, Andreeasson bound, and surface redshift was examined (Figures 16–19). The gravitational mass function is regular (free from singularity) at

the core and gradually increases from the center towards the boundary surface of the star where $(r = \widetilde{x})$. The compactification factor obeys Buchdahl condition [135] and does not cross the allowable range (4/9) for the mass to radius ratio. It is finite at every interior point of the star and positively increases from the center towards the surface area. The inequality $P_r - \mu + 2P_t$ has been satisfied Andreeasson bound for charged compact sphere. We have determined that the inequality is negative inside the stellar object and remains negative at every interior point of the star. From Figure 19, we studied the evolutionary nature of surface redshift with their respective $f(R)$ models. It suggested that the evolution is positive and attains maximum allowable value ($\approx 0.55$) at the boundary of the star where $(r = \widetilde{x})$. Hence, the present results suggest that our proposed compact star object should be a strange quark star.

In the present scenario, we explored the new viable solutions of charged strange star models with the strange matter MIT bag model EoS along with KB type metric ansatz in the background of so-called $f(R)$ gravity. From this study, we obtained a wide family of solutions for our proposed compact object. The solutions are free of central singularity, physically realistic, and stable in the entire distribution of the fluid sphere. Conclusively, we expect that our presented celestial object is an ultradense strange quark star and quite fit with two specific viable $f(R)$ models at the theoretical and the astrophysical scales. Moreover, in future, we will try to find out these results in other alternative theories of gravity such as $f(R,T)$, $f(R,G)$, and $f(T)$ theories of gravity.

## Data Availability

The data used to support the findings of this study are available from the corresponding author upon request.

## Conflicts of Interest

The authors declare that they have no conflicts of interest.

## References


[1] A. G. Riess, A. V. Filippenko, P. Challis et al., "Observational evidence from supernovae for an accelerating universe and a cosmological constant," *The Astronomical Journal*, vol. 116, p. 1009, 1998.

[2] S. Perlmutter, G. Aldering, G. Goldhaber et al., "Measurements of omega and lambda from 42 high-redshift supernovae," *The Astrophysical Journal*, vol. 517, p. 565, 1999.

[3] P. Astier, J. Guy, N. Regnault et al., "Creating a legacy and learning about dark energy," *Astronomy & Astrophysics*, vol. 447, p. 31, 2006.

[4] A. G. Riess, L.-G. Strolger, J. Tonry et al., "Type Ia Supernova discoveries at z>1 from the hubble space telescope: evidence for past deceleration and constraints on dark energy evolution," *The Astrophysical Journal*, vol. 607, pp. 665–687, 2004.

[5] A. G. Riess, L.-G. Strolger, S. Casertano et al., "New hubble space telescope discoveries of type Ia Supernovae at z > 1: narrowing constraints on the early behavior of dark energy," *The Astrophysical Journal*, vol. 659, p. 98, 2007.

[6] D. N. Spergel, "Three-year Wilkinson Microwave Anisotropy Probe (WMAP) observations: implications for cosmology," *The Astrophysical Journal Supplement Series*, vol. 170, p. 377, 2007.

[7] W. M. Wood-Vasey, G. Miknaitis, C. W. Stubbs et al., "Observational constraints on the nature of the dark energy: first cosmological results from the ESSENCE supernova survey," *The Astrophysical Journal*, vol. 666, p. 694, 2007.

[8] M. Kowalski, D. Rubin, G. Aldering et al., "Improved cosmological constraints from new, old and combined supernova datasets," *The Astrophysical Journal*, vol. 686, p. 749, 2008.

[9] E. Komatsu, J. Dunkley, M. R. Nolta et al., "Five-year Wilkinson microwave anisotropy probe observations: cosmological interpretation," *The Astrophysical Journal Supplement Series*, vol. 180, p. 330, 2009.

[10] C. L. Bennett, M. Halpern, G. Hinshaw et al., "First-year Wilkinson Microwave Anisotropy Probe (WMAP) observations: preliminary maps and basic results," *The Astrophysical Journal Supplement Series*, vol. 148, p. 1, 2003.

[11] D. N. Spergel, L. Verde, H. V. Peiris et al., "First-year Wilkinson Microwave Anisotropy Probe (WMAP) observations: determination of cosmological parameters," *The Astrophysical Journal Supplement Series*, vol. 148, p. 175, 2003.

[12] M. Tegmark, M. A. Strauss, M. R. Blanton et al., "Cosmological parameters from SDSS and WMAP," *Physical Review D*, vol. 69, Article ID 103501, 2004.

[13] K. Abazajian, A. McCarthy, K. Jennifer et al., "The first data release of the sloan digital sky survey," *The Astronomical Journal*, vol. 126, p. 2081, 2003.

[14] K. Abazajian, A. McCarthy, K. Jennifer et al., "The second data release of the sloan digital sky survey," *The Astronomical Journal*, vol. 128, p. 502, 2004.

[15] K. Abazajian, A. McCarthy, K. Jennifer et al., "The third data release of the sloan digital sky survey," *The Astronomical Journal*, vol. 129, p. 1755, 2005.

[16] E. Hawkins, S. Maddox, S. Cole et al., "The 2dF Galaxy Redshift survey: correlation functions, peculiar velocities and the matter density of the universe," *Monthly Notices of the Royal Astronomical Society*, vol. 346, p. 78, 2003.

[17] L. Verde, A. F. Heavens, W. J. Percival et al., "The 2dF Galaxy Redshift Survey: the bias of galaxies and the density of the universe," *Monthly Notices of the Royal Astronomical Society*, vol. 335, p. 432, 2002.

[18] D. J. Eisentein, I. Zehavi, D. W. Hogg et al., "Detection of the Baryon Acoustic Peak in the large-scale correlation function of SDSS luminous red galaxies," *The Astrophysical Journal*, vol. 633, p. 560, 2005.

[19] S. Nojiri and S. D. Odintsov, "Unified cosmic history in modified gravity: from $f(R)$ theory to Lorentz non-invariant models," *Physics Reports*, vol. 505, p. 59, 2011.

[20] S. Nojiri and S. D. Odintsov, "Introduction to modified gravity and gravitational alternative for dark energy," *International Journal of Geometric Methods in Modern Physics*, vol. 4, p. 115, 2007.

[21] K. Bamba, S. Capozziello, S. i. Nojiri, and S. D. Odintsov, "Dark energy cosmology: the equivalent description via different theoretical models and cosmography tests," *Astrophysics and Space Science*, vol. 342, no. 1, p. 155, 2012.

[22] S. Capozziello, "Curvature quintessence," *International Journal of Modern Physics D*, vol. 11, no. 4, p. 483, 2002.

[23] T. Harko, F. S. N. Lobo, S. Nojiri, and S. D. Odintsov, "$f(R, T)$ gravity," *Physical Review D*, vol. 84, Article ID 024020, 2011.

[24] S. D. Odintsov and D. Saez-Gomez, "$f(R, T, R_{\mu\nu}T^{\mu\nu})$ gravity phenomenology and ΛCDM universe," *Physics Letters B*, vol. 725, p. 437, 2013.

[25] Z. Haghani, T. Harko, F. S. N. Lobo, H. R. Sepangi, and S. Shahidi, "Further matters in space-time geometry: $f(R, T, R_{\mu\nu}T^{\mu\nu})$ gravity," *Physical Review D*, vol. 88, Article ID 044023, 2013.

[26] I. Ayuso, J. B. Jimenez, and A. de la Cruz-Dombriz, "Consistency of universally nonminimally coupled $f(R, T, R^{\mu\nu} T^{\mu\nu})$ theories," *Physical Review D*, vol. 91, Article ID 104003, 2015.

[27] G. Cognola, E. Elizalde, S. Nojiri, S. D. Odintsov, and S. Zerbini, "Dark energy in modified Gauss-Bonnet gravity: late-time acceleration and the hierarchy problem," *Physical Review D*, vol. 73, Article ID 084007, 2006.

[28] A. Azadi, D. Momeni, and M. Nouri-Zonoz, "Cylindrical solutions in metric $f(R)$ gravity," *Physics Letters B*, vol. 670, p. 210, 2008.

[29] S. Capozziello, I. De Martino, S. D. Odintsov, and A. Stabile, "Hydrostatic equilibrium and stellar structure in $f(R)$-gravity," *Physical Review D*, vol. 83, Article ID 064004, 2011.

[30] S. Capozziello, M. De Laurentis, I. De Martino, M. Formisano, and S. D. Odintsov, "Jeans analysis of self-gravitating systems in *f(R)* gravity," *Physical Review D*, vol. 85, Article ID 044022, 2012.

[31] M. Jamil, F. M. Mahomed, and D. Momeni, "Reconstruction of some cosmological models in $f(R, T)$ cosmology," *Physics Letters B*, vol. 702, p. 315, 2011.

[32] S. H. Hendi and D. Momeni, "Black-hole solutions in $F(R)$ gravity with conformal anomaly," *European Physical Journal C*, vol. 71, p. 1823, 2011.

[33] D. Momeni and H. Gholizade, "A note on constant curvature solutions in cylindrically symmetric metric $f(R)$ gravity," *International Journal of Modern Physics D*, vol. 18, no. 11, p. 1719, 2009.

[34] M. U. Farooq, M. Jamil, D. Momeni, and R. Myrzakulov, "Reconstruction of $f(T)$ and $f(R)$ gravity according to $(m, n)$-type holographic dark energy," *Canadian Journal of Physics*, vol. 91, no. 9, p. 703, 2013.

[35] D. Momeni, M. Raza, and R. Myrzakulov, "Construction of a holographic superconductor in $F(R)$ gravity," *The European Physical Journal Plus*, vol. 129, p. 30, 2014.

[36] M. J. S. Houndjo, M. E. Rodrigues, N. S. Mazhari, D. Momeni, and R. Myrzakulov, "Higher-derivative $f(R, R, T)$ theories of gravity," *International Journal of Modern Physics D*, vol. 26, no. 3, Article ID 1750024, 2017.

[37] D. Psaltis, "Constraining Brans-Dicke gravity with accreting millisecond pulsars in ultracompact Binaries," *The Astrophysical Journal*, vol. 688, no. 2, p. 1282, 2008.

[38] F. Briscese, E. Elizalde, S. Nojiri, and S. D. Odintsov, "Phantom scalar dark energy as modified gravity: understanding the origin of the Big Rip singularity," *Physics Letters B*, vol. 646, no. 2-3, p. 105, 2007.

[39] S. Tsujikawa, T. Tamaki, and R. Tavakol, "Chameleon scalar fields in relativistic gravitational backgrounds," *Journal of Cosmology and Astroparticle Physics*, vol. 5, p. 20, 2009.

[40] S. Arapoglu, C. Deliduman, and K. Y. Eksi, "Constraints on perturbative *f(R)* gravity via neutron stars," *Journal of Cosmology and Astroparticle Physics*, vol. 7, p. 20, 2011.

[41] H. Alavirad and J. M. Weller, "Modified gravity with logarithmic curvature corrections and the structure of relativistic stars," *Physical Review D*, vol. 88, Article ID 124034, 2013.

[42] A. V. Astashenok, "Neutron star models in frames of *f(R)* gravity," *AIP Conference Proceedings*, vol. 1606, p. 99, 2014.

[43] A. V. Astashenok, S. Capozziello, and S. D. Odintsov, "Maximal neutron star mass and the resolution of the hyperon puzzle in modified gravity," *Physical Review D*, vol. 89, Article ID 103509, 2014.

[44] A. V. Astashenok, S. Capozziello, and S. D. Odintsov, "Extreme neutron stars from Extended Theories of Gravity," *Journal of Cosmology and Astroparticle Physics*, vol. 1, 2015.

[45] A. V. Astashenok, S. Capozziello, and S. D. Odintsov, "Magnetic neutron stars in $f(R)$ gravity," *Astrophysics and Space Science*, vol. 355, no. 2, p. 333, 2015.

[46] S. S. Yazadjiev, D. D. Doneva, K. D. Kokkotas, and K. V. Staykov, "Non-perturbative and self-consistent models of neutron stars in $R$-squared gravity," *Journal of Cosmology and Astroparticle Physics*, vol. 2014, no. 6, p. 003, 2014.

[47] E. Egeland, *Compact Stars*Trondheim, Norway, 2007.

[48] S. Capozziello, M. De Laurentis, R. Farinelli, and S. D. Odintsov, "Mass-radius relation for neutron stars in *f(R)* gravity," *Physical Review D*, vol. 93, Article ID 023501, 2016.

[49] C. Alcock, E. Farhi, and A. Olinto, "Strange stars," *The Astrophysical Journal*, vol. 310, p. 261, 1986.

[50] P. Haensel, J. L. Zdunik, and R. Schaeffer, "Strange quark stars," *Astronomy & Astrophysics*, vol. 160, p. 121, 1986.

[51] M. F. Shamir and I. Fayyaz, "Effect of $f(R)$-Gravity models on compact stars," *Theoretical and Mathematical Physics*, vol. 202, no. 1, p. 112, 2020.

[52] M. F. Shamir and A. Malik, "Behavior of anisotropic compact stars in $f(R, \phi)$ gravity," *Communications in Theoretical Physics*, vol. 71, no. 5, p. 599, 2019.

[53] Z. Yousaf, M. Sharif, M. Ilyas, and M. Z. Bhatti, "Influence of *f(R)* models on the existence of anisotropic self-gravitating systems," *European Physical Journal C*, vol. 77, p. 691, 2017.

[54] G. Abbas, M. Zubair, and G. Mustafa, "Anisotropic strange quintessence stars in $f(R)$ gravity," *Astrophysics and Space Science*, vol. 358, p. 26, 2015.

[55] M. Zubair and G. Abbas, "Possible formation of compact stars in $f(R, T)$ gravity," *Astrophysics and Space Science*, vol. 361, p. 342, 2016.

[56] R. A. Sussman and L. G. Jaime, "Lemaître-Tolman-Bondi dust solutions in $f(R)$ gravity," *Classical and Quantum Gravity*, vol. 34, no. 24, Article ID 245004, 2017.

[57] H. Shabani and A. H. Ziaie, "Consequences of energy conservation violation: late time solutions of $\Lambda(T)$CDM subclass of $f(R, T)$ gravity using dynamical system approach," *European Physical Journal C*, vol. 77, p. 31, 2017.

[58] R. Garattini and G. Mandanici, "Influence of $f(R)$ models on the existence of anisotropic self-gravitating systems," *European Physical Journal C*, vol. 77, p. 57, 2017.

[59] P. K. Sahoo, P. Sahoo, and B. K. Bishi, "Anisotropic cosmological models in f(R,T) gravity with variable deceleration parameter," *International Journal of Geometric Methods in Modern Physics*, vol. 14, no. 6, Article ID 1750097, 2017.

[60] S. K. Sahu, S. K. Tripathy, P. K. Sahoo, and A. Nath, "Cosmic transit and anisotropic models in $f(R, T)$ gravity," *Chinese Journal of Physics*, vol. 55, no. 3, p. 862, 2017.

[61] S. K. Maurya and F. Tello-Ortiz, "Charged anisotropic compact star in $f(R, T)$ gravity: a minimal geometric deformation gravitational decoupling approach," *Physics of the Dark Universe*, vol. 27, Article ID 100442, 2020.

[62] S. K. Maurya and F. Tello-Ortiz, "Decoupling gravitational sources by MGD approach in Rastall gravity," *Physics of the Dark Universe*, vol. 29, Article ID 100577, 2020.

[63] M. Sharif and S. Saba, "Embedding class-1 anisotropic solution in $f(G)$ gravity," *Chinese Journal of Physics*, vol. 64, p. 374, 2020.

[64] M. Ilyas, "Charged compact stars in $f(G)$ gravity," *European Physical Journal C*, vol. 78, p. 757, 2018.

[65] M. Zubair and G. Abbas, "Possible formation of compact stars in $f(R, T)$ gravity," *Astrophysics and Space Science*, vol. 361, p. 27, 2016.

[66] M. Zubair, G. Abbas, and I. Noureen, "Possible formation of compact stars in $f(R, T)$ gravity," *Astrophysics and Space Science*, vol. 361, p. 8, 2016.

[67] M. Zubair, I. H. Sardar, F. Rahaman, and G. Abbas, "Interior solutions of fluid sphere in $f(R, T)$ gravity admitting conformal killing vectors," *Astrophysics and Space Science*, vol. 361, p. 238, 2016.

[68] G. Abbas, S. Qaisar, and M. A. Meraj, "Anisotropic strange quintessence stars in $f(T)$ gravity," *Astrophysics and Space Science*, vol. 357, p. 156, 2015.

[69] G. Abbas, S. Qaisar, and A. Jawad, "Strange stars in $f(T)$ gravity with MIT bag model," *Astrophysics and Space Science*, vol. 359, p. 57, 2015.

[70] S. S. Bayin, "Anisotropic fluid spheres in general relativity," *Physical Review D*, vol. 26, p. 1262, 1982.

[71] M. Cosenza, L. Herrera, M. Esculpi, and L. Witten, "Some models of anisotropic spheres in general relativity," *Journal of Mathematical Physics*, vol. 22, no. 1, p. 118, 1981.

[72] T. Harko and M. K. Mak, "Anisotropic charged fluid spheres in $D$ space–time dimensions," *Journal of Mathematical Physics*, vol. 41, p. 4752, 2000.

[73] T. Harko and M. K. Mak, "Anisotropic relativistic stellar models," *Annalen der Physik*, vol. 11, no. 1, p. 3, 2002.

[74] M. K. Mak and T. Harko, "Quark stars admitting a one-parameter group of conformal motions," *International Journal of Modern Physics D*, vol. 13, p. 149, 2004.

[75] M. Kalam, F. Rahaman, S. Ray, S. M. Hossein, I. Karar, and J. Naskar, "Anisotropic strange star with de Sitter spacetime," *European Physical Journal C*, vol. 72, p. 2248, 2012.

[76] M. Kalam, F. Rahaman, S. M. Hossein, and S. Ray, "Central density dependent anisotropic compact stars," *European Physical Journal*, vol. C73, p. 2409, 2013.

[77] S. M. Hossein, F. Rahaman, J. Naskar, M. Kalam, and S. Ray, "Anisotropic compact stars with variable cosmological constant," *International Journal of Modern Physics D*, vol. 21, no. 13, Article ID 1250088, 2012.

[78] P. Bhar, F. Rahaman, S. Ray, and V. Chatterjee, "Possibility of higher-dimensional anisotropic compact star," *European Physical Journal C*, vol. 75, p. 190, 2015.

[79] P. Bhar, "A new hybrid star model in Krori-Barua space-time," *Astrophysics and Space Science*, vol. 357, p. 46, 2015.

[80] K. N. Singh, R. K. Bisht, S. K. Maurya, and N. Pant, "Static fluid spheres admitting Karmarkar condition," *Chinese Physics C*, vol. 44, Article ID 035101, 2020.

[81] K. N. Singh, A. Ali, F. Rahaman, and S. Nasri, "Compact stars with exotic matter," *Physics of the Dark Universe*, vol. 29, Article ID 100575, 2020.

[82] N. Sarkar, S. Sarkar, K.. N. Singh, and F. Rahaman, "Relativistic compact stars with dark matter density profile," *European Physical Journal C*, vol. 80, p. 255, 2020.

[83] A. Errehymy and M. Daoud, "Studies an analytic model of a spherically symmetric compact object in Einsteinian gravit," *European Physical Journal C*, vol. 80, p. 258, 2020.

[84] S. Rosseland, "Electrical state of a star," *Monthly Notices of the Royal Astronomical Society*, vol. 84, p. 720, 1924.

[85] S. Ray, A. L. Espindola, M. Malheiro, J. P. S. Lemos, and V. T. Zanchin, "Electrically charged compact stars and formation of charged black holes," *Physical Review D*, vol. 68, Article ID 084004, 2003.

[86] C. R. Ghezzi, "Relativistic structure, stability, and gravitational collapse of charged neutron stars," *Physical Review D*, vol. 72, Article ID 104017, 2005.

[87] F. Rahaman, R. Sharma, S. Ray, R. Maulick, and I. Karar, "Strange stars in Krori-Barua space-time," *European Physical Journal C*, vol. 72, p. 2071, 2012.

[88] S. K. Maurya, Y. K. Gupta, S. Ray, and D. Deb, "A new model for spherically symmetric charged compact stars of embedding class 1," *European Physical Journal C*, vol. 77, p. 45, 2017.

[89] S. Thirukkanesh and S. D. Maharaj, "Charged anisotropic matter with a linear equation of state," *Classical and Quantum Gravity*, vol. 25, no. 23, Article ID 235001, 2008.

[90] M. Esculpi and E. Alomá, "Conformal anisotropic relativistic charged fluid spheres with a linear equation of state," *The European Physical Journal C*, vol. 67, no. 3-4, p. 521, 2010.

[91] E. F. Eiroa and C. Simeone, "Stability of charged thin shells," *Physical Review D*, vol. 83, Article ID 104009, 2011.

[92] A. Hewish, S. J. Bell, J. D. H. Pilkington, P. F. Scott, and R. A. Collins, "Observation of a rapidly pulsating radio source," *Nature*, vol. 217, no. 5130, p. 709, 1968.

[93] S. L. Shapiro and S. A. Teukolosky, *Black Holes, White Dwarfs and Neutron Stars: The Physics of Compact Objects*, Wiley, New York, NY, USA, 1983.

[94] E. Witten, "Cosmic separation of phases," *Physical Review D*, vol. 30, p. 272, 1984.

[95] E. Farhi and R. L. Jaffe, "Strange matter," *Physical Review D*, vol. 30, no. 11, p. 2379, 1984.

[96] K. D. Krori and J. Barua, "A singularity-free solution for a charged fluid sphere in general relativity," *Journal of Physics A: Mathematical and General*, vol. 8, no. 4, p. 508, 1975.

[97] K. S. Cheng, Z. G. Dai, and T. Lu, "Strange stars and related astrophysical phenomena," *International Journal of Modern Physics D*, vol. 7, no. 2, p. 139, 1998.

[98] A. Chodos, R. L. Jaffe, K. Johnson, C. B. Thorn, and V. F. Weisskopf, "New extended model of hadrons," *Physical Review D*, vol. 9, no. 12, p. 3471, 1974.

[99] H. Reissner, "Über die Eigengravitation des elektrischen Feldes nach der Einsteinschen Theorie," *Annalen der Physik*, vol. 355, no. 9, p. 106, 1916.

[100] G. Nordstrom, "On the energy of the Gravitational field in Einstein's theory," in *Proceedings of the Koninklijke Nederlandse Akademie van Wetenschappen/C*, vol. 20, p. 1238, 1918.

[101] G. H. Bordbar, H. Bahri, and F. Kayanikhoo, "Calculation of the structural properties of a strange quark star in the presence of a strong magnetic field using a density dependent bag constant," *Research in Astronomy and Astrophysics*, vol. 12, no. 9, p. 1280, 2012.

[102] A. A. Starobinsky, "A new type of isotropic cosmological models without singularity," *Physics Letters B*, vol. 91, p. 99, 1980.

[103] M. Sharif and Z. Yousaf, "Effects of CDTT model on the stability of spherical collapse in Palatini $f(R)$ gravity," *European Physical Journal C*, vol. 73, p. 2633, 2013.

[104] H. R. Kausar and I. Noureen, "Dissipative spherical collapse of charged anisotropic fluid in $f(R)$ gravity," *European Physical Journal C*, vol. 74, p. 2760, 2014.

[105] S. Chakrabarti, R. Goswami, S. D. Maharaj, and N. Banerjee, "Conformally flat collapsing stars in $f(R)$ gravity," *General Relativity and Gravitation*, vol. 50, p. 148, 2018.
[106] H. Nazar and G. Abbas, "Charged anisotropic collapsing stars with heat flux in $f(R)$ gravity," *Chinese Journal of Physics*, vol. 63, p. 436, 2020.
[107] M. Ruderman, "Pulsars: structure and dynamics," *Annual Review of Astronomy and Astrophysics*, vol. 10, no. 1, p. 427, 1972.
[108] N. K. Glendenning, *Compact Stars: Nuclear Physics, Particle Physics and General Relativity*, p. 468, Springer, New York, NY, USA, 1997.
[109] M. Herzog and F. K. Ropke, "Three-dimensional hydrodynamic simulations of the combustion of a neutron star into a quark star," *Physical Review D*, vol. 84, Article ID 083002, 2011.
[110] S. Biswas, D. Shee, S. Ray, F. Rahaman, and B. K. Guha, "Relativistic strange stars in Tolman-Kuchowicz spacetime," *Annals of Physics*, vol. 409, Article ID 167905, 2019.
[111] C. W. Misner and D. H. Sharp, "Relativistic equations for adiabatic, spherically symmetric gravitational collapse," *Physical Review*, vol. 136, no. 2, pp. 571–576, 1964.
[112] D. Shee, S. Ghosh, F. Rahaman, B. K. Gupta, and S. Ray, "Compact star in pseudo-spheroidal spacetime," *Astrophysics and Space Science*, vol. 362, p. 114, 2017.
[113] H. Quevedo, "General static axisymmetric solution of Einstein s vacuum field equations in prolate spheroidal coordinates," *Physical Review D*, vol. 39, p. 2904, 1989.
[114] E. N. Chifu, "Gravitational fields exterior to homogeneous spheroidal masses," *Abra. Zelm. J.*vol. 5, p. 31, 2012.
[115] K. V. Staykov, D. D. Doneva, S. S. Yazadjiev, S. S. Yazadjiev, and K. D. Kokkotas, "Slowly rotating neutron and strange stars in R2 gravity," *Journal of Cosmology and Astroparticle Physics*, vol. 2014, no. 10, p. 6, 2014.
[116] M. Malaver, *Frontiers in Applied Mathematics and Statistics*, vol. 1, p. 9, 2014.
[117] S. A. Ngubelanga, S. D. Maharaj, and S. Ray, *Astrophysics and Space Science*, vol. 357, p. 74, 2015.
[118] D. Shee, F. Rahaman, B. K. Gupta, and S. Ray, "Anisotropic stars with non-static conformal symmetry," *Astrophysics and Space Science*, vol. 361, p. 167, 2016.
[119] J. R. Oppenheimer and G. M. Volkoff, "On massive neutron cores," *Physical Review*, vol. 55, no. 4, p. 374, 1939.
[120] J. Ponce de Leon, "Static anisotropic fluid spheres in general relativity with nonuniform density," *General Relativity and Gravitation*, vol. 19, p. 797, 1987.
[121] Ponce de Le, J. on, Limiting configurations allowed by the energy conditions," *General Relativity and Gravitation*, vol. 25, p. 1123, 1993.
[122] M. K. Gokhroo and A. L. Mehra, "Anisotropic spheres with variable energy density in general relativity," *General Relativity and Gravitation*, vol. 26, no. 1, p. 75, 1994.
[123] D. Deb, S. R. Chowdhury, S. Ray, F. Rahaman, and B. K. Guha, "Relativistic model for anisotropic strange stars," *Annals of Physics*, vol. 387, p. 239, 2017.
[124] L. Herrera, G. J. Ruggeri, and L. Witten, "Adiabatic contraction of anisotropic spheres in general relativity," *The Astrophysical Journal*, vol. 234, p. 1094, 1979.
[125] L. Herrera, "Cracking of self-gravitating compact objects," *Physics Letters A*, vol. 165, p. 206, 1992.
[126] R. Chan, L. Herrera, and N. O. Santos, "Dynamical instability for radiating anisotropic collapse," *Monthly Notices of the Royal Astronomical Society*, vol. 265, no. 3, p. 533, 1993.
[127] H. Abreu, H. Hernandez, and L. A. Nunez, "Sound speeds, cracking and the stability of self-gravitating anisotropic compact objects," *Classical and Quantum Gravity*, vol. 24, p. 4631, 2007.
[128] Andr, H. easson, Sharp bounds on the critical stability radius for relativistic charged spheres," *Communications in Mathematical Physics*, vol. 288, pp. 715–730, 2009.
[129] B. K. Harrison, K. S. Thorne, M. Wakano, and J. A. Wheeler, *Gravitational Theory and Gravitational Collapse*, University of Chicago Press, Chicago, IL, USA, 1965.
[130] Zel, Y. B. dovich and I. D. Novikov, *Relativistic Astrophysics 1, Stars and Relativity*, University of Chicago Press, Chicago, IL, USA, 1971.
[131] W. Hillebrandt and K. O. Steinmetz, "Anisotropic neutron star models: stability against radial and nonradial pulsations," *Astronomy & Astrophysics*, vol. 53, p. 283, 1976.
[132] H. Bondi, "The contraction of gravitating spheres," *Proceedings of the Royal Society of London Series A*, vol. 281, p. 39, 1964.
[133] H. Heintzmann and W. Hillebrandt, "Neutron stars with an anisotropic equation of state: mass, redshift and stability," *Astronomy & Astrophysics*, vol. 24, p. 51, 1975.
[134] R. Chan, L. Herrera, and N. O. Santos, "Dynamical instability for radiating anisotropic collapse," *Monthly Notices of the Royal Astronomical Society*, vol. 265, no. 3, p. 533, 1993.
[135] H. A. Buchdahl, "General relativistic fluid spheres," *Physical Review*, vol. 116, no. 4, p. 1027, 1959.
[136] M. K. Mak, P. N. Dobson, and T. Harko, "Maximum mass-radius ratios for charged compact general relativistic objects," *Europhysics Letters*, vol. 55, no. 3, p. 310, 2001.
[137] D. E. Barraco and V. H. Hamity, *Physical Review D*, vol. 65, Article ID 124028, 2002.
[138] B. V. Ivanov, *Physical Review D*, vol. 65, Article ID 104001, 2002.
[139] C. G. Böhmer and T. Harko, "Bounds on the basic physical parameters for anisotropic compact general relativistic objects," *Classical and Quantum Gravity*, vol. 23, no. 22, p. 6479, 2006.